Study of Time-Like Nucleon Form Factors at BESIII

Samer Ahmed

on behalf of the BESIII Collaboration

Electromagnetic Interactions with Nucleons and Nuclei
30.10.2019, Cyprus

Outline

- **Introduction of the electromagnetic form factors**
- **Measurements of the electromagnetic form factors of nucleon:**
  - **Proton form factors**
  - **Neutron form factors $\Rightarrow$ Results are shown for the first time.**
- **Summary**

Electromagnetic Form Factors of the Nucleon

- **The Form factors (FFs)** characterize the internal structure and dynamics of the nucleon.

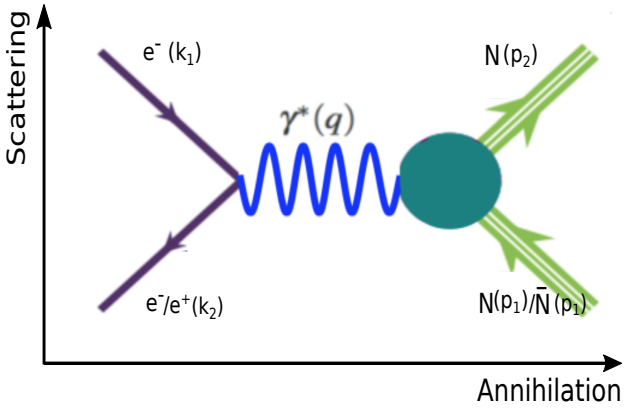

- Scattering amplitude in Born approximation:

$$\mathcal{M} = \frac{1}{q^2}\,[e\,\bar{u}(k_2)\gamma_\mu u(k_1)]\,\underbrace{[e\,\bar{U}(p_2)\Gamma^\mu(p_1,p_2)U(p_1)]}_{\text{Nucleon EM 4-current: } J_N^\mu}$$

- The electromagnetic vertex of nucleon:

$$\Gamma^\mu = \gamma^\mu F_1^N(q^2) + \frac{i\sigma^\mu_\nu q^\nu}{2M} F_2^N(q^2)$$

$F_1^N(q^2)$: **Dirac FF.**

$F_2^N(q^2)$: **Pauli FF.**

- Combination of Pauli and Dirac FFs leads to the so called **Sachs FFs:**

$$G_E = F_1(q^2) + (q^2/4M^2)F_2(q^2) \qquad G_M = F_1(q^2) + F_2(q^2)$$

How experimentally the Form Factors are determined?

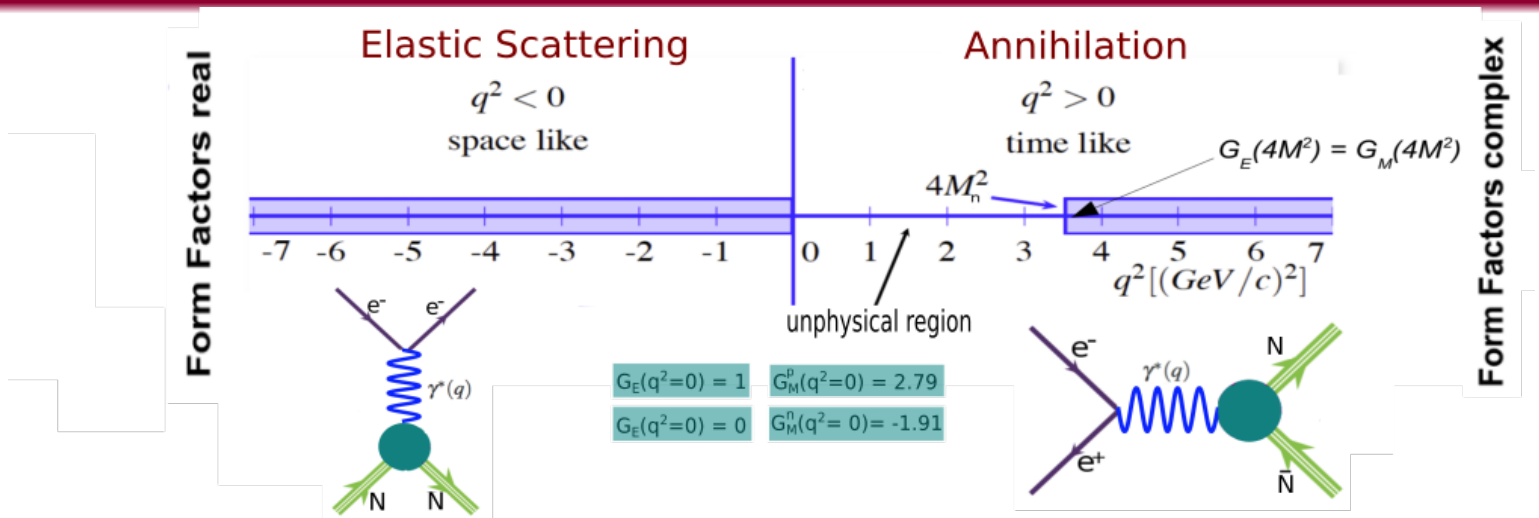

Electromagnetic Form Factors in Time-Like Region

Direct Scan Method:

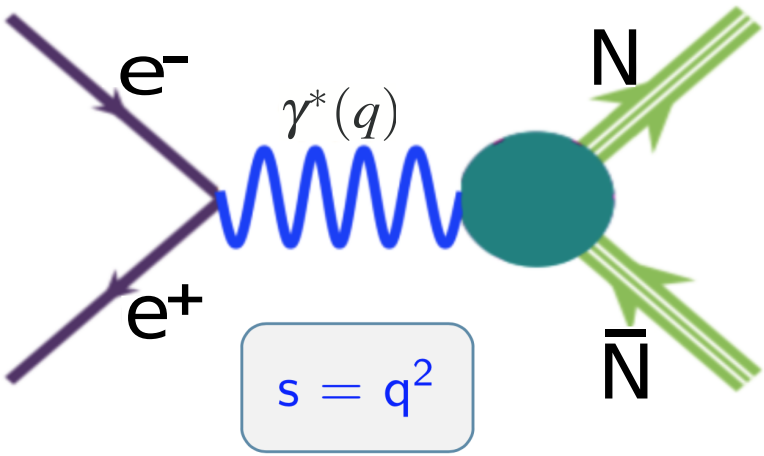

- Beam energy is discrete.
- Luminosity is relatively small.

$$\left(\frac{d\sigma_{N\bar{N}}}{d\Omega}\right) = \frac{\alpha^2 C\beta}{4q^2}\left[|G_M^N|^2(1+cos^2\theta) + \frac{1}{\tau}|G_E^N|^2(1-cos^2\theta)\right]$$

- q^2 is single at each beam energy.

Initial State Radiation Method:

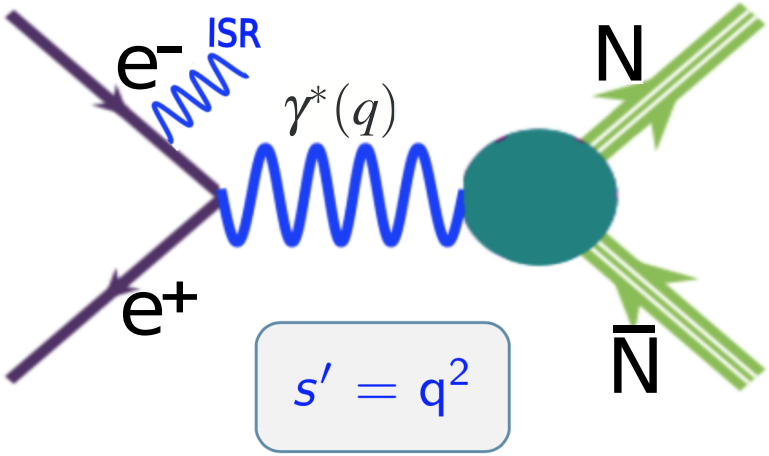

$$s' = x \cong 2E_\gamma/\sqrt{s}$$

- Beam energy is fixed.
- Luminosity is relatively high.

$$\left(\frac{d^2\sigma_{N\bar{N}\gamma}}{dq^2 d\theta}\right) = \frac{1}{q^2} W(q^2, x, \theta_\gamma)\sigma_{N\bar{N}}(q^2)$$

$$W(q^2, x, \theta_\gamma) = \frac{\alpha}{\pi x}\left(\frac{2-2x+x^2}{sin^2\theta_\gamma} - \frac{x^2}{2}\right)$$

- q^2 is continuous from threshold to s.

Status of the Proton Form Factors

Proton Form Factors in the Time-Like Region

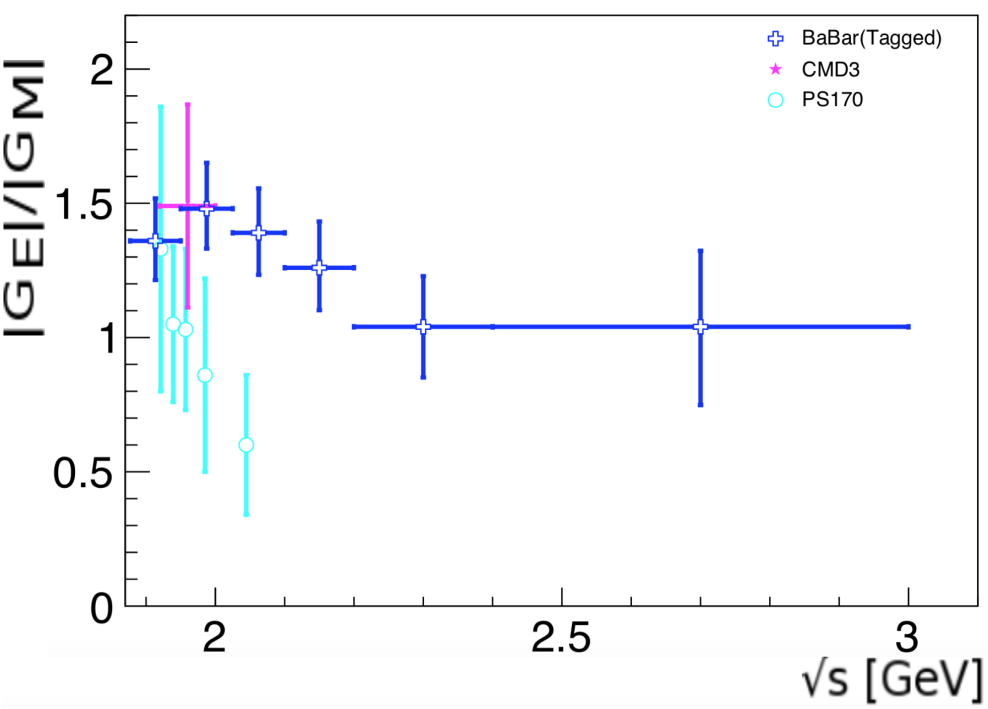

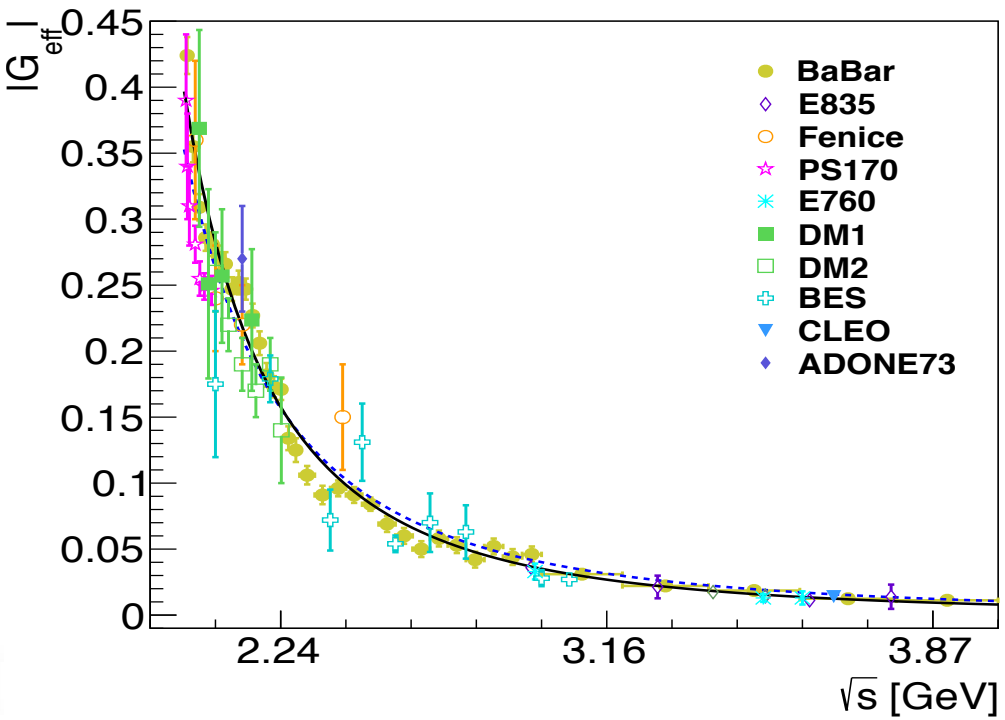

Existing results for the proton form factors before the contribution of BESIII

- **The proton form factor ratio $|G_E|/|G_M|$ had been measured by 2 experiments only.**
- **The results from the two experiments are inconsistent. Which one is correct?.**
- Due to the low statistics, only the effective form factor is measured in most experiments.

Measurements of Proton Form Factors at BESIII

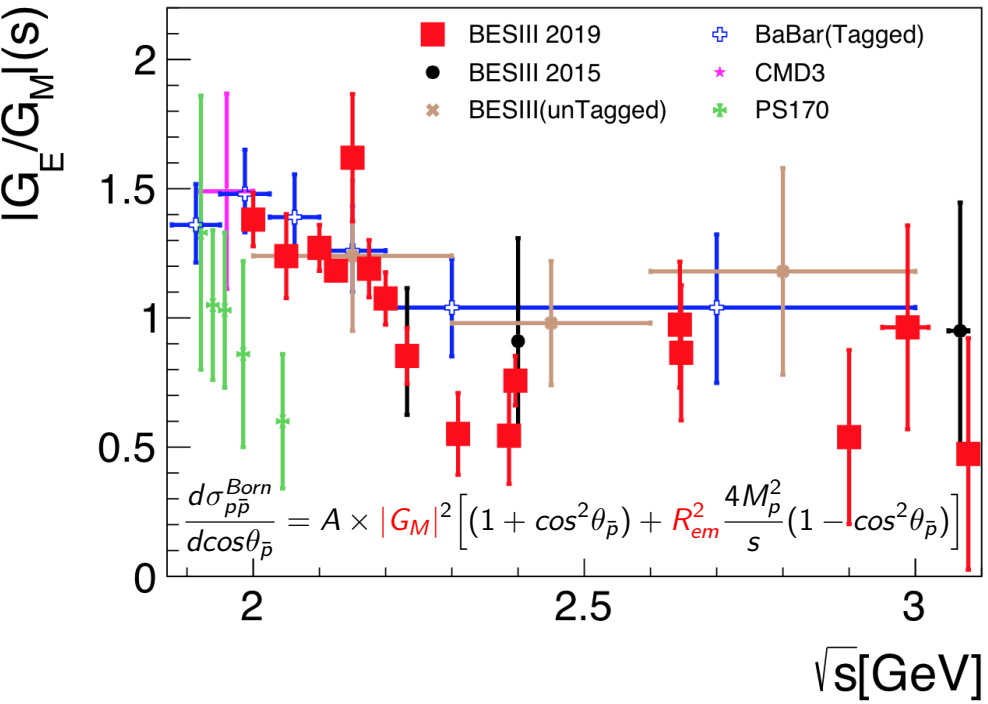

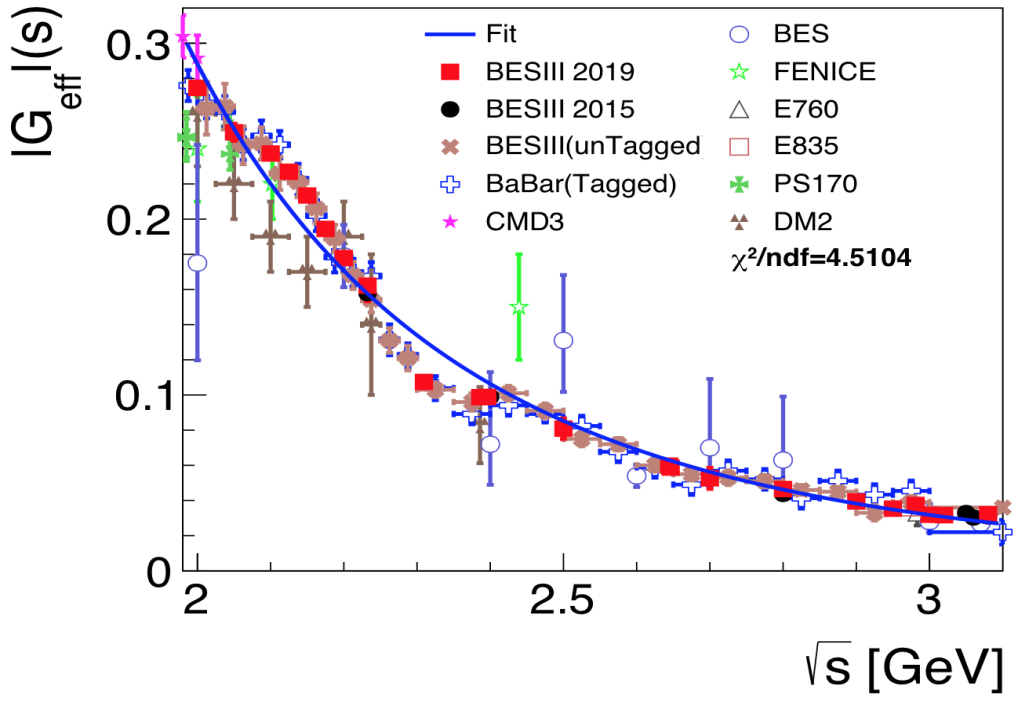

BESIII results for the $e^+e^- \to p\bar{p}$ cross section and effective form factors

- Direct scan method:
  - 2012 data, 156.7 pb^{-1}, 12 c.m energies, Phys. Rev. D 91, 112004 (2015)
  - 2015 data, 668.5 pb^{-1}, 22 c.m energies, arXiv:1905.09001 $\Longrightarrow$ most precise results.
- Initial state radiation method:
  - Untagged analysis: data at [3.773 - 4.60 GeV], 7.4 pb^{-1}, Phys. Rev. D 99, 092002.
  - Tagged analysis: data at [3.773 - 4.60 GeV], 7.4 pb^{-1}, under review.

Measurements of Proton Form Factors at BESIII

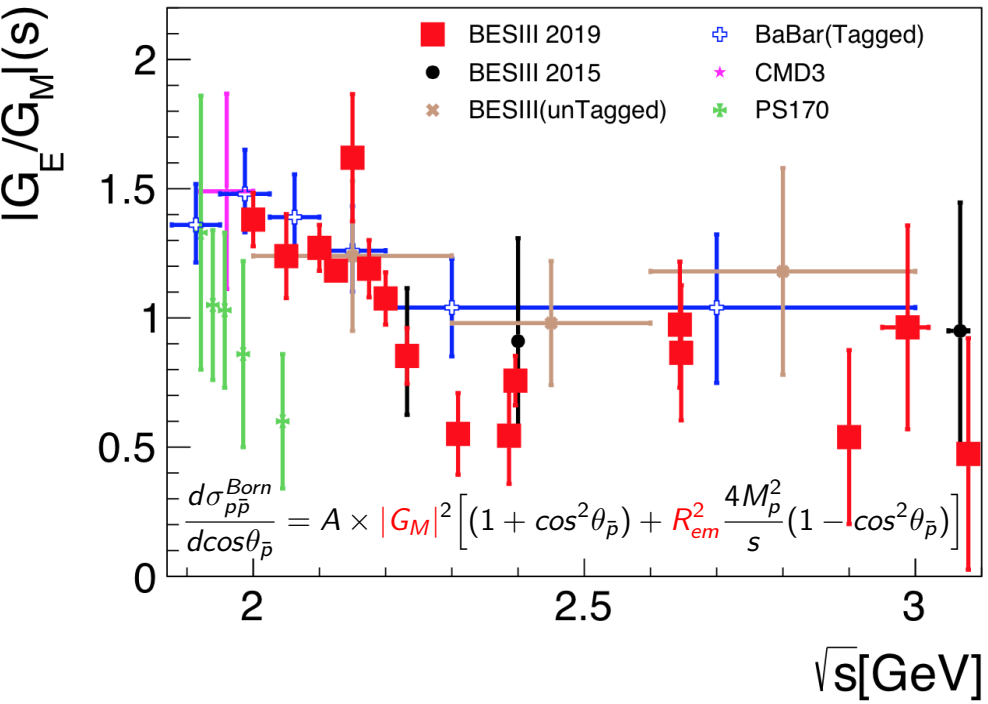

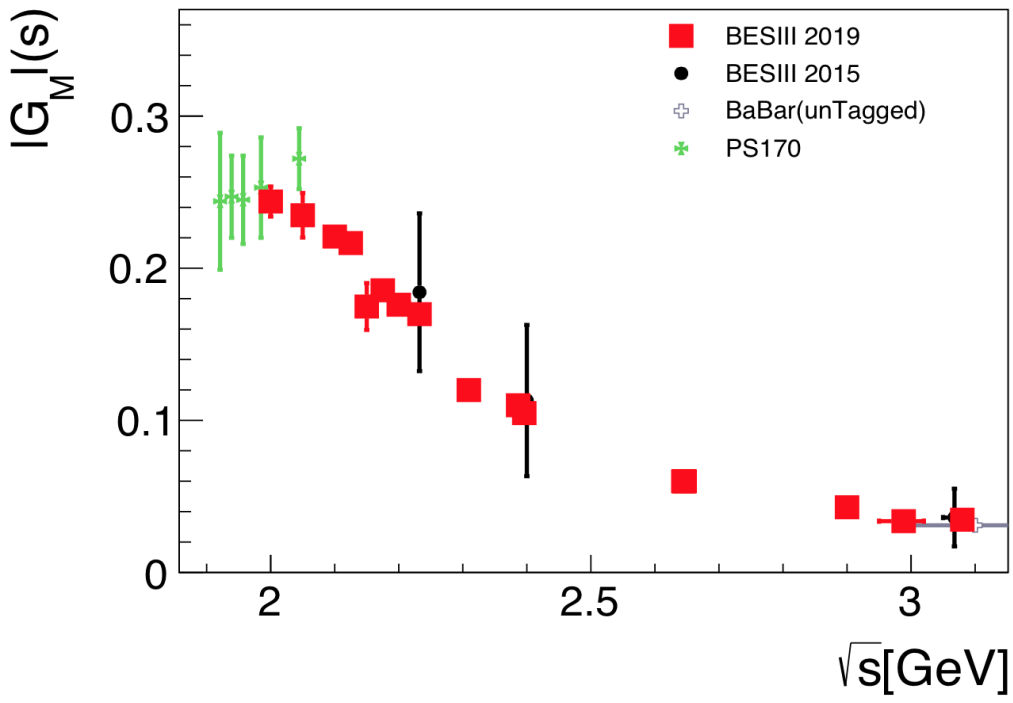

BESIII results for the $e^+e^- \rightarrow p\bar{p}$ cross section and effective form factors

- **The BESIII results are consistent with the BaBar measurement.**
- **The precision of the BESIII results is significantly improved.**

Status of the Neutron Form Factors

New results

Neutron Form Factors in the Space- and Time-Like Region

- **The electric and magnetic FFs had been measured in the SL region while not in the TL region.**

Space-Like region **Time-Like region**

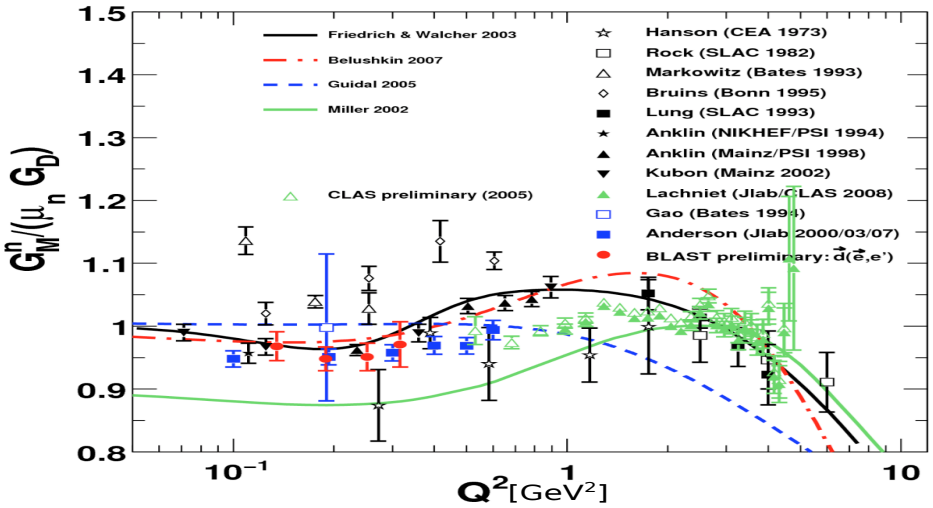

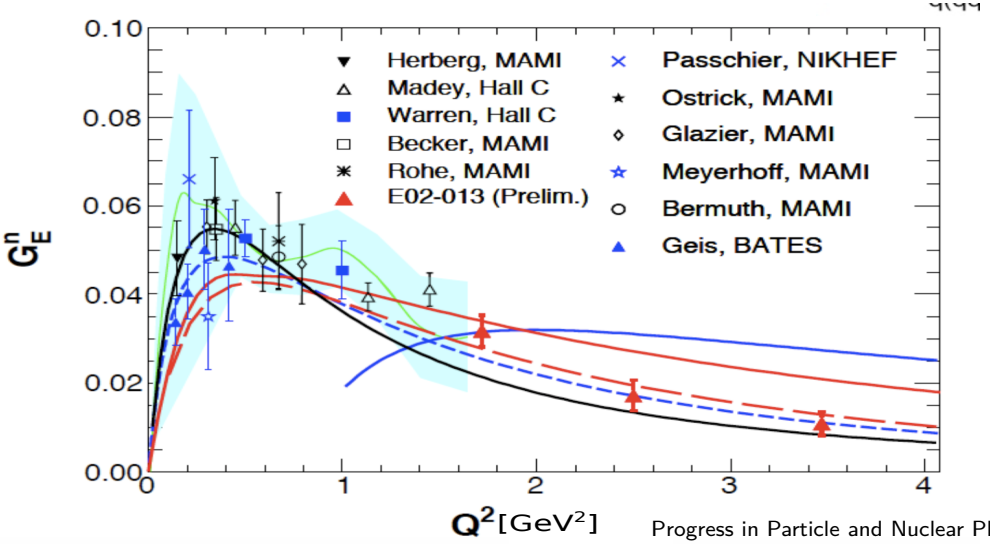

No results for the neutron FFs (G_E^n and G_M^n).

Progress in Particle and Nuclear Physics 59 (2007) 694-764.

Motivation 1

- **For a complete understanding of the nucleon structure:**
  - **The electromagnetic form factors of the neutron in the Time-Like region should be measured.**
- **The only available results for neutron are the effective form factor but with poor precision.**
- The results from FENICE experiment show an unexpected behavior (twice as large as for the proton).
- **Many models exist to describe the neutron structure. Which is the most precise one?**
- **The pQCD predicts asymptotic behavior for the Space-Like (SL) and Time-Like (TL) results:**
  - **Can we provide the necessary results for a test?**

Motivation 2

- **Large data sets with a total luminosity of 651 pb^{-1} in the range [2.0, 3.08] GeV have been used.**
- **The neutron form factors G_E^n and G_M^n have been determined for the first time.**
- **Details about the analysis can be found in the backup and in the poster session by Samer Ahmed.**

Results for Born Cross Section and Effective Form Factor

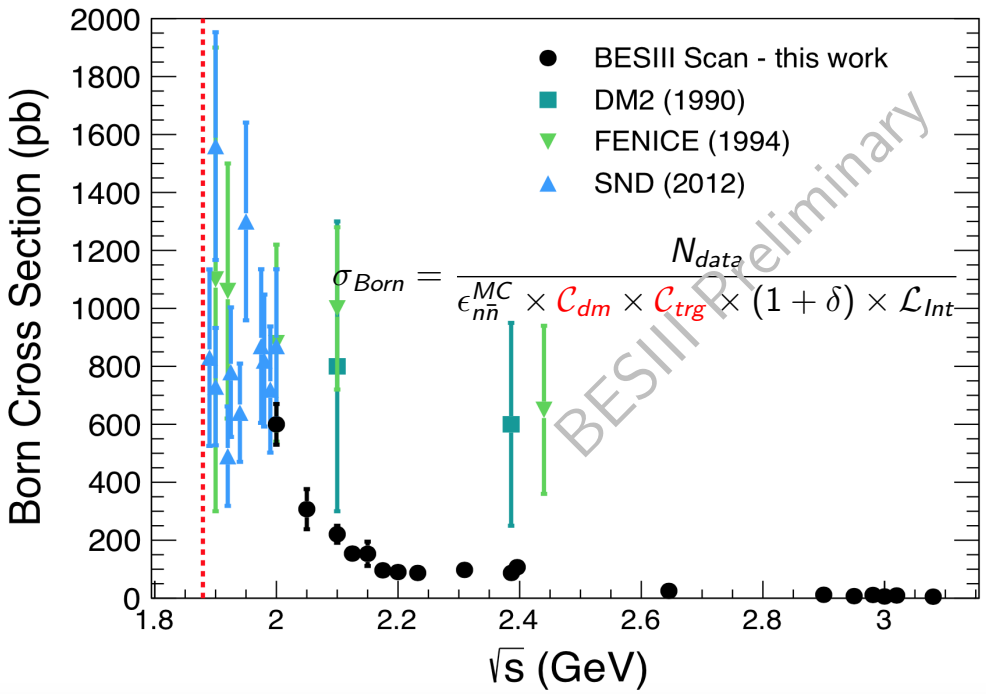

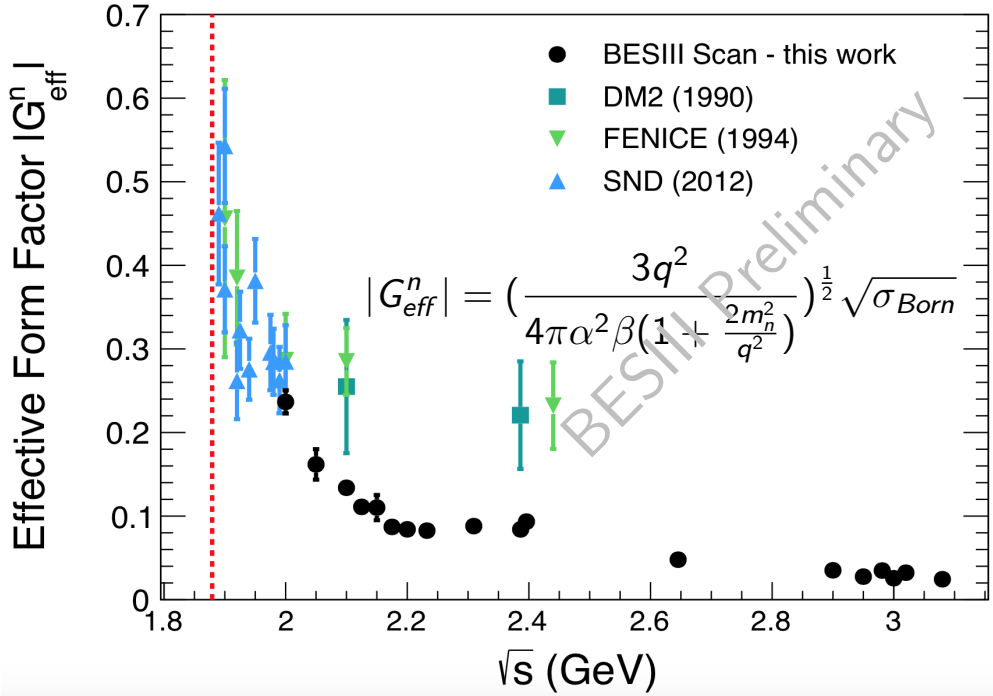

Results of the $e^+e^- \to n\bar{n}$ Born Cross Section:

- **The Born cross sections are determined in a wide range of $\sqrt{s}$ with unprecedented precisions.**
- **The best precision among all analyzed $\sqrt{s}$ is achieved at $\sqrt{s}$= 2.396 GeV to be 7.3%.**
- The cross section at $\sqrt{s}$= 2.0 GeV is in agreement with the FENICE and the SND results.
- **The cross section at $\sqrt{s}$= 2.396 GeV differs by around 2σ with the FENICE result.**

Born Cross Section of the $e^+e^- \to n\bar{n}$ and $p\bar{p}$ Processes

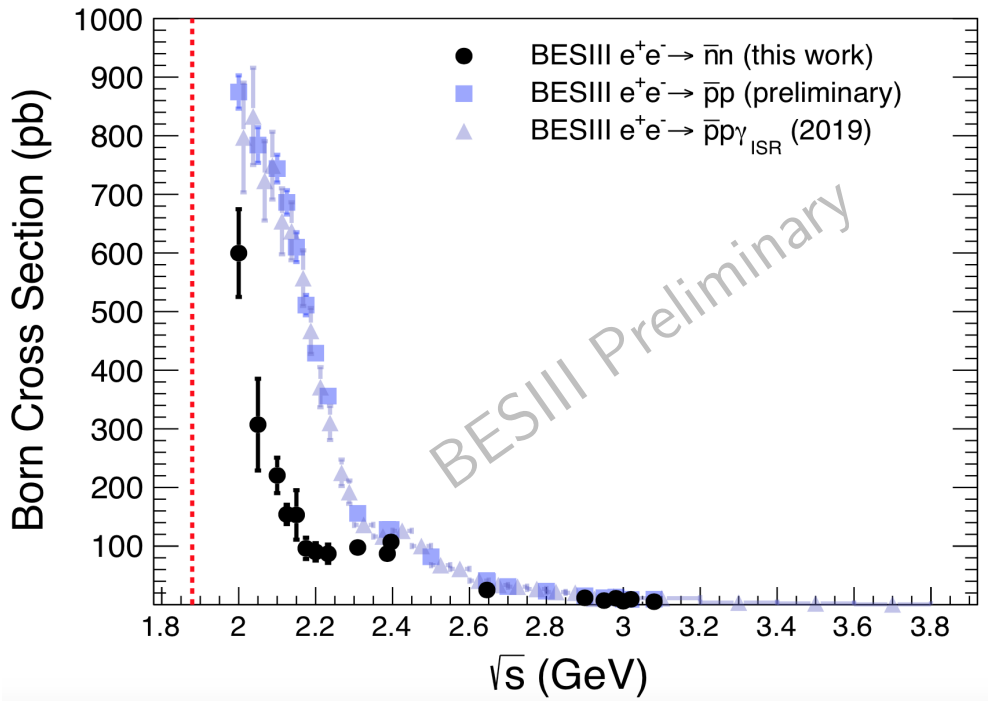

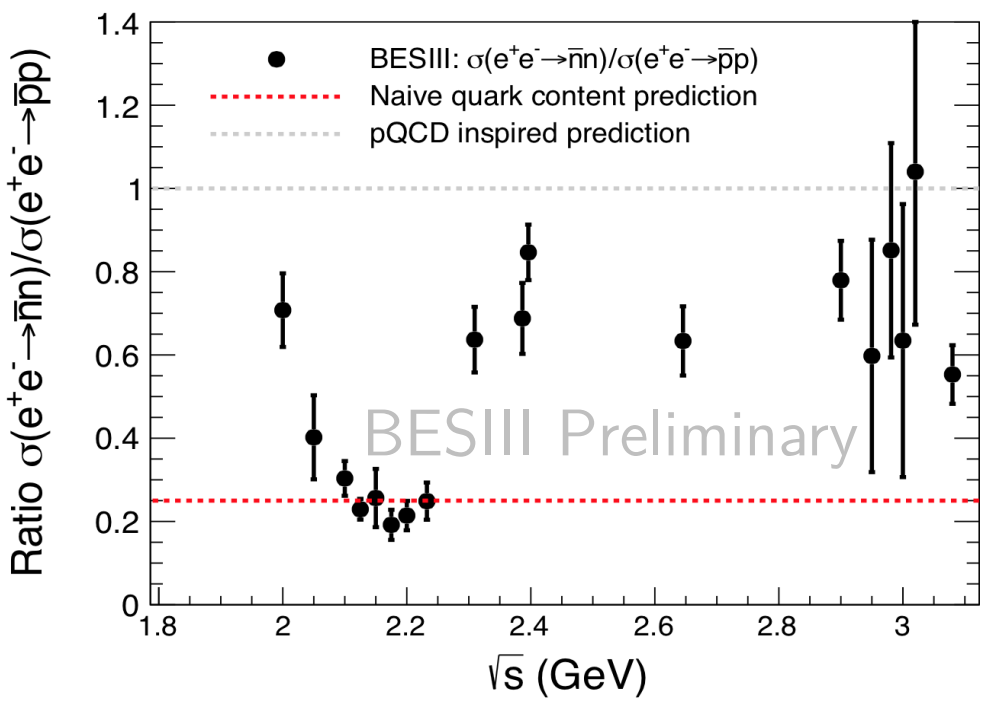

Comparison of the $e^+e^- \to n\bar{n}$ and $e^+e^- \to p\bar{p}$ Cross Sections:

- **The Born cross sections of the $n\bar{n}$ and $p\bar{p}$ processes are roughly similar at $\sqrt{s} > 2.4$ GeV.**
- The ratio $R_{np} = \sigma^{e^+e^- \to n\bar{n}}_{Born} / \sigma^{e^+e^- \to p\bar{p}}_{Born}$ shows an interesting behaviour over the range of $\sqrt{s}$:
  - The pQCD predicts the $R_{np} < 1$. The ratio is predicted as $R_{np} \simeq |q_d/q_u|^2 \simeq 0.25$ by [†].
  - **The BESIII results for the cross section ratio don't agree with the FENICE results ($R_{np} > 1$).**

[†] V. L. Chernyak and A. R. Zhitnitsky, Phys. Rept. 112, 173 (1984).

Comparison of the Effective Form Factor of Baryon

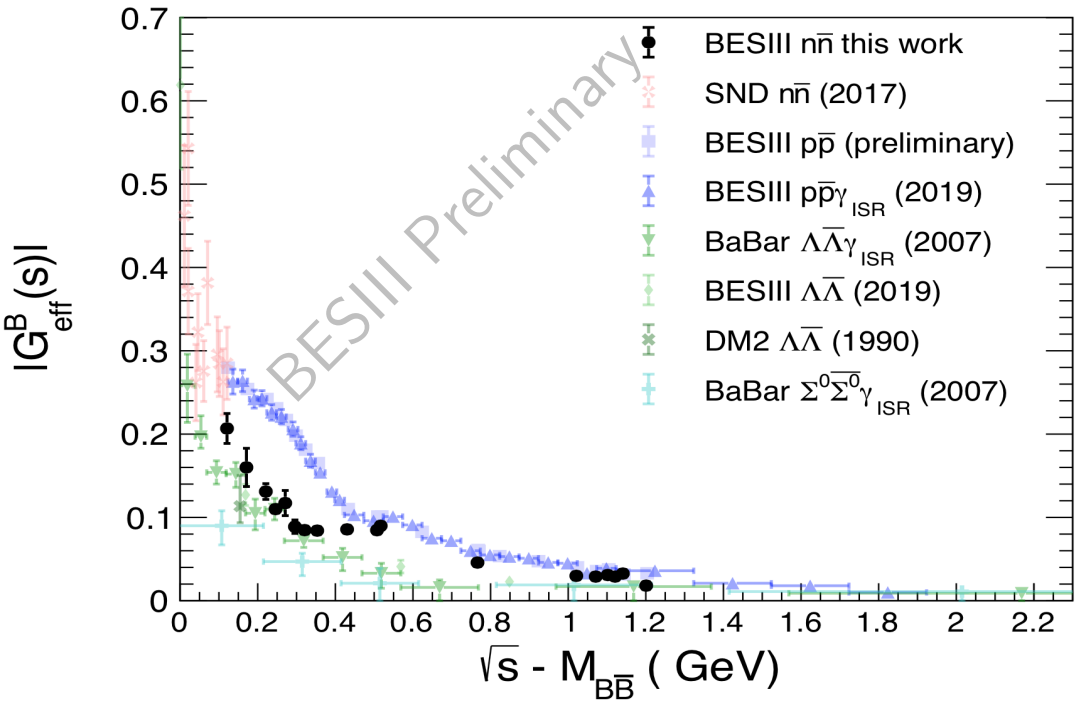

Results for the Effective Form Factor of Baryon:

- The results for the effective form factor of neutron are compared to those of the other baryons.
- **The results for the neutron effective form factor show step behavior in the range [0.3 - 0.6] GeV.**

Oscillation Behavior in the Effective Form Factor

- An oscillation in the effective form factor of proton is observed by BaBar and then confirmed by BESIII.
- **What about the effective form factor of the neutron? Does an oscillation exist?**

$$F_{osc} = |G_{eff}^{n,p}(q^2)| - G_D(q^2), \quad q^2 = s$$

$$G_D(q^2) = \mathcal{A} \cdot \frac{1}{(1 - \frac{q^2}{0.71(GeV)^2})^2} \cdot \frac{1}{(1 + \frac{q^2}{m_a^2})}$$

- The normalisation $\mathcal{A}$ is extracted by a fit to the effective FF of the neutron:

$$\mathcal{A} = 4.86 \pm 0.09$$

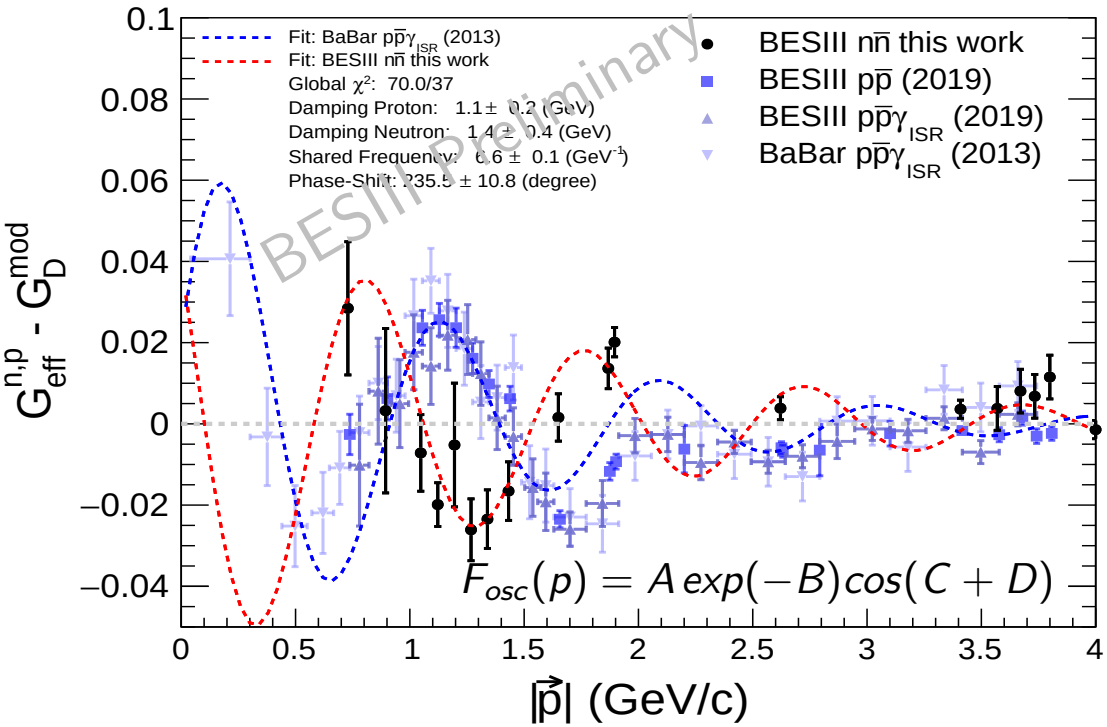

- **An oscillation behavior is observed in the effective form factor of the neutron.**
- **The oscillation is observed with a relative phase shift of $\sim 235^\circ \pm 11^\circ$ compare to that for the proton.**

|p| is the relative momentum of the final state particles.

Results for the Neutron Electromagnetic Form Factors

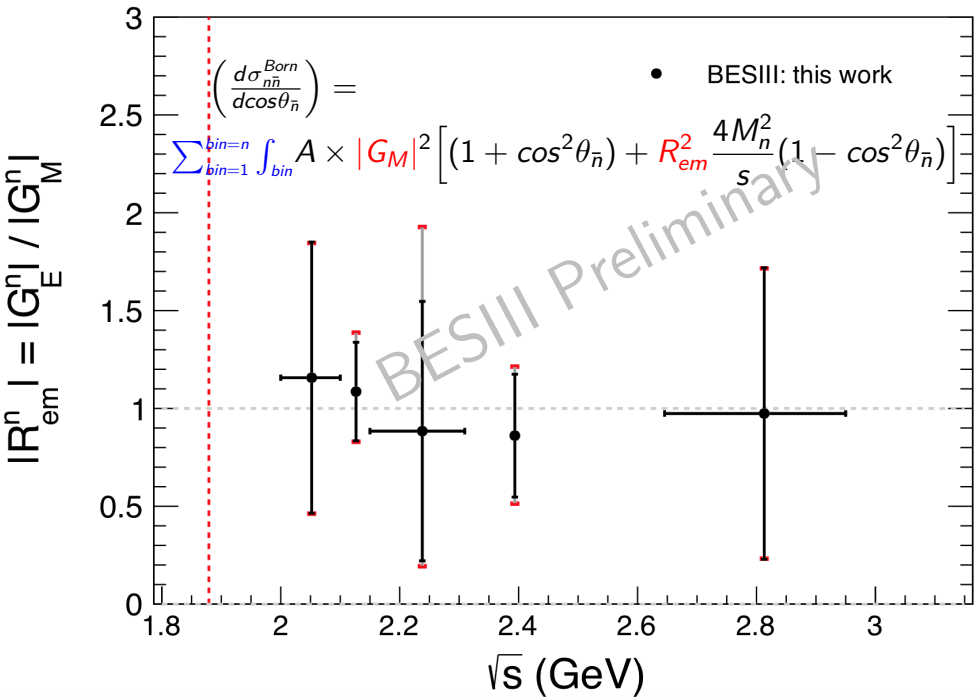

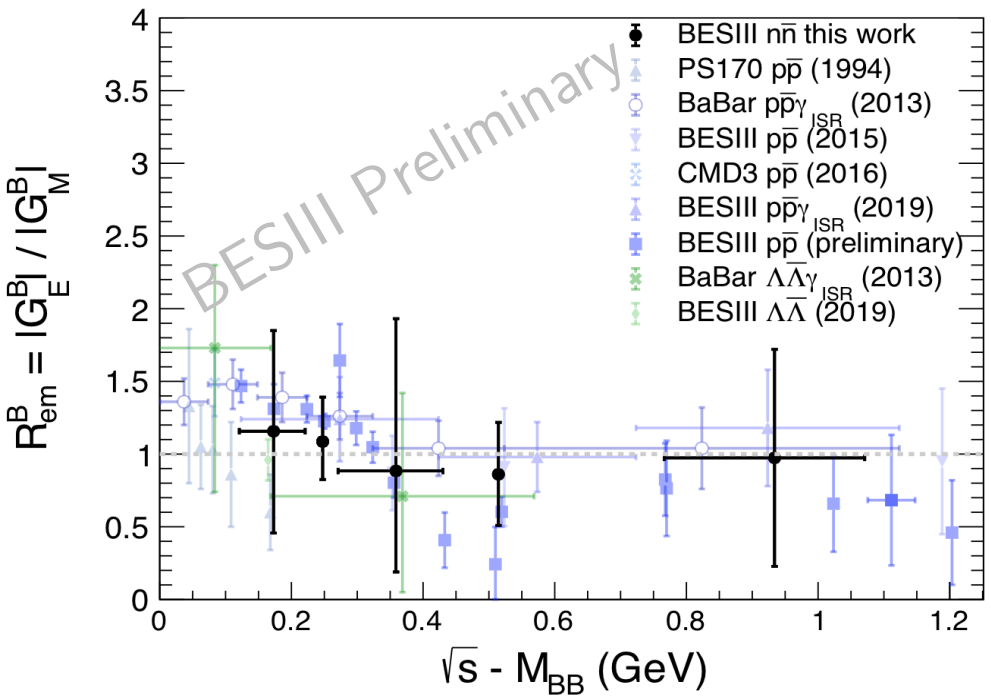

Results for the Neutron Time-like Form Factors at BESIII:

- **The neutron form factor ratio R_{em} has been determined for the first time in the TL region.**
- **The uncertainty of the extracted results for the form factor ratio is dominated by the statistical one.**
- **The statistical precision of the R_{em} is 35.7% and 52.2% at $\sqrt{s}$= 2.125 and $\sqrt{s}$= 2.394 GeV.**

Black and grey colors in the left plot are statistical and systematical uncertainties while red is the combined uncertainties.

Results for the Magnetic Form Factor of the Neutron

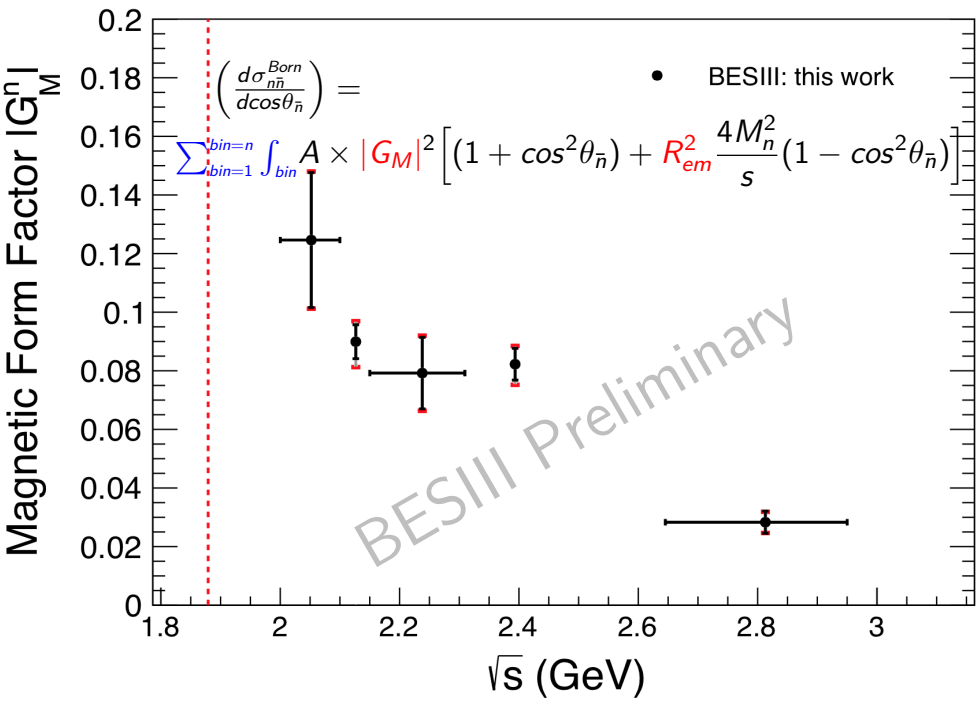

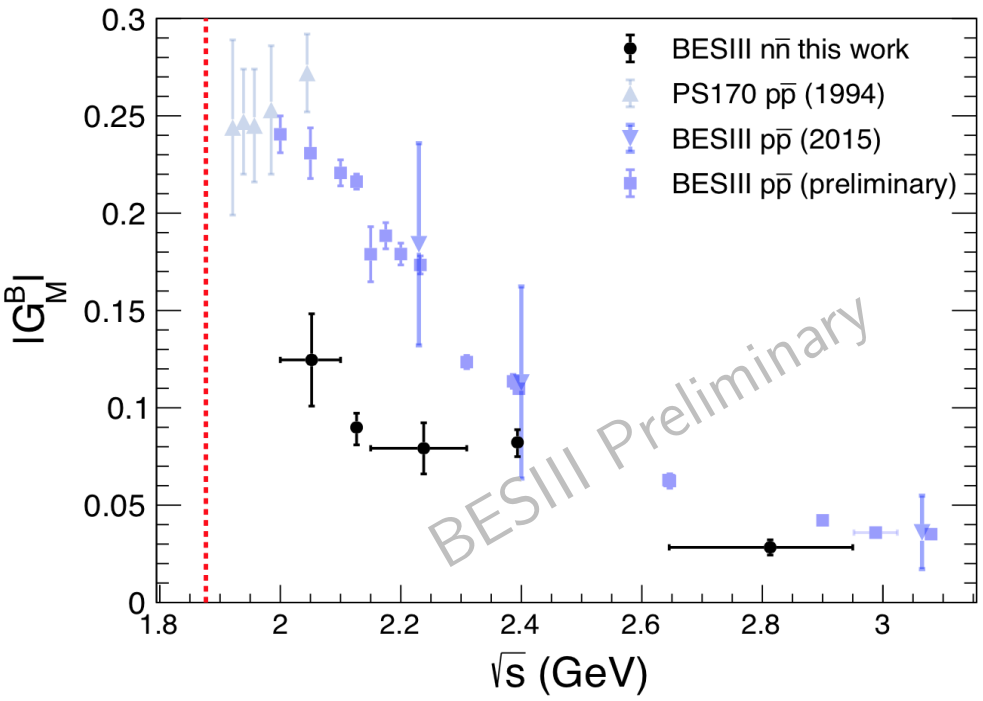

Results for the Magnetic Form Factor of the Neutron ($|G_M|$):

- **The magnetic form factor has been determined for the first time in the TL region at $\sqrt{s}$>2.0 GeV.**
- **The uncertainties of the magnetic form factor results are dominated by the statistical one.**
- **The statistical precision of the $|G^n_M|$ is 9.5% and 7.1% at $\sqrt{s}$= 2.125 and $\sqrt{s}$= 2.394 GeV.**

Black and grey colors are statistical and systematical uncertainties while red is the combined uncertainties.

Results for the Magnetic Form Factor of the Neutron

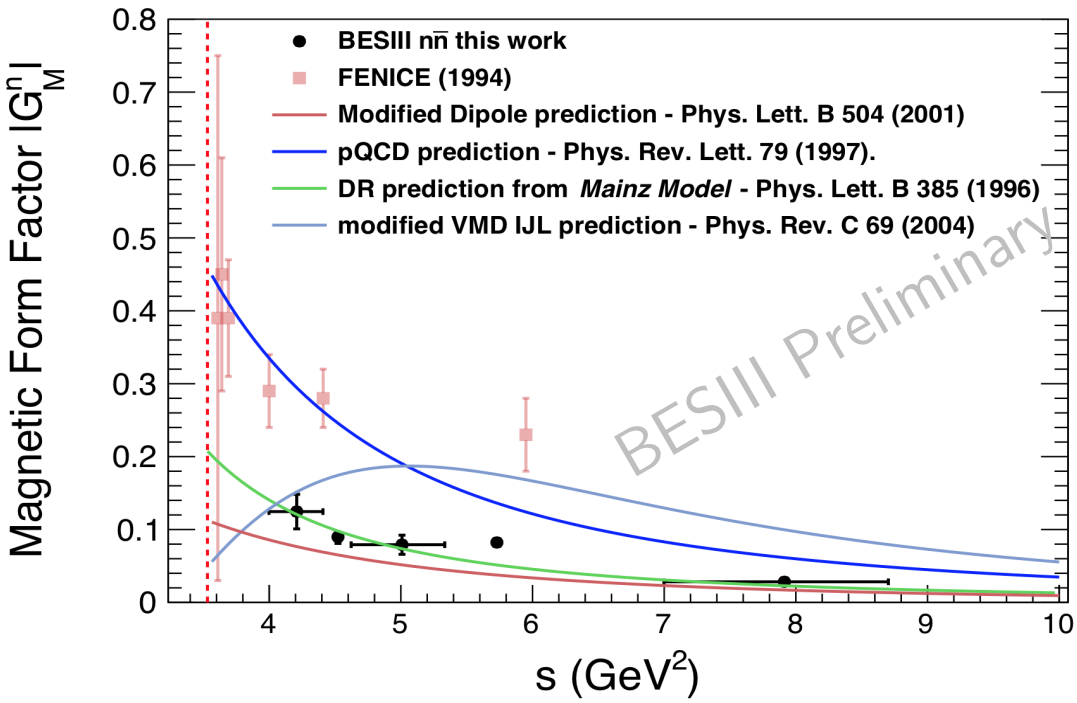

Comparison of the Magnetic Form Factor Results to the Theoretical Predictions:

- The only existing results for $|G_M^n|$ are from FENICE, they were determined under the hypothesis $|G_E^n| = 0$.
- **The $|G_M^n|$ results from this analysis are well described by the Mainz model based on dispersion relations.**

Comparison of Nucleon Form Factors in SL and TL Regions

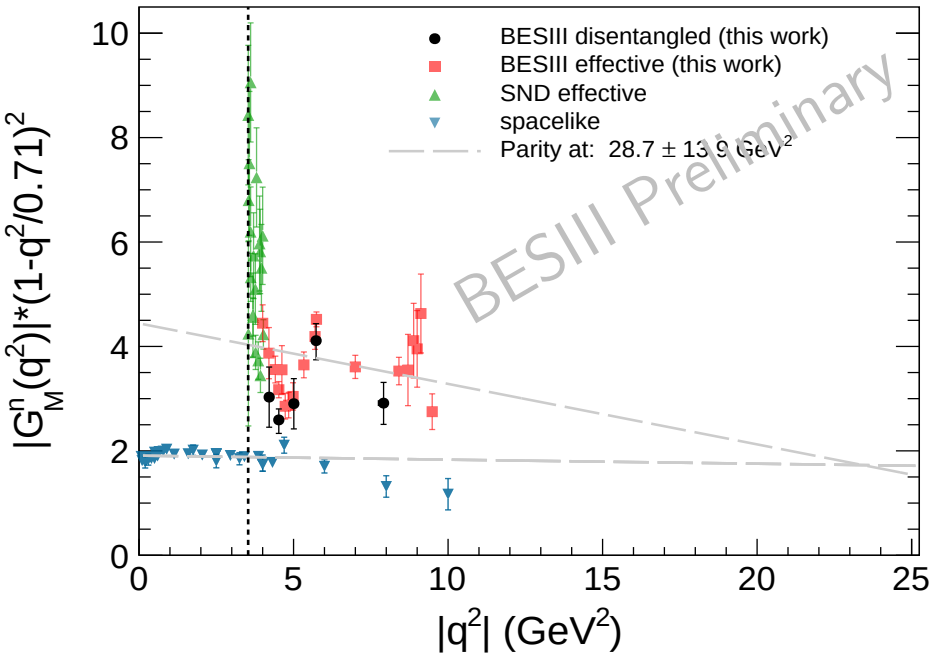

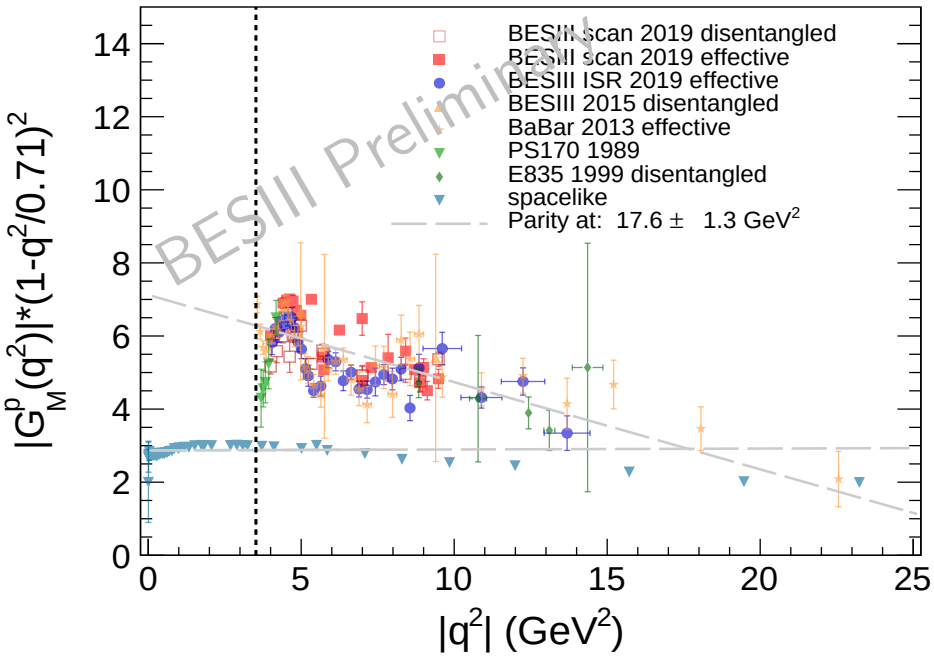

Neutron and Proton Magnetic Form Factors in the SL and TL Regions:

- **The pQCD predicts an asymptotic behavior of the form factors in the SL and TL regions:**
  - **At high q^2, the pQCD predicts $G_M(SL) = G_M(TL)$ for neutron and proton form factors.**
- **The neutron and proton form factors in the TL region are larger than those in the SL region.**

The representation of y-axis shows the deviation from the dipole behavior $(1/[1 - q^2/0.71GeV^2)^2]$.

Summary

- The BESIII experiment provides an excellent opportunity to measure the nucleon FFs.
- The cross section of the $e^+e^- \rightarrow p\bar{p}$ process has been measured in a wide range of q^2.
- **The proton form factors (G_M and R_{em}) are measured with unprecedented precision.**
- The cross section of the $e^+e^- \rightarrow n\bar{n}$ process has been determined in a wide range of q^2.
- **The results for the cross section of the $e^+e^- \rightarrow n\bar{n}$ process are significantly improved.**
- **The effective form factor of the neutron is determined at 18 c.m. energies.**
- **An oscillation behaviour in the effective form factor of the neutron is observed.**
- **The results for the neutron FFs (R_{em} and G_M) have been determined for the first time.**
- **A comparison between the results from this work and several predications is performed.**
- **The results for the time-like neutron form factors are presented for the first time.**

Thank you

Backup

Analysis Strategy for the Extraction of Neutron Form Factors

Analysis Strategy

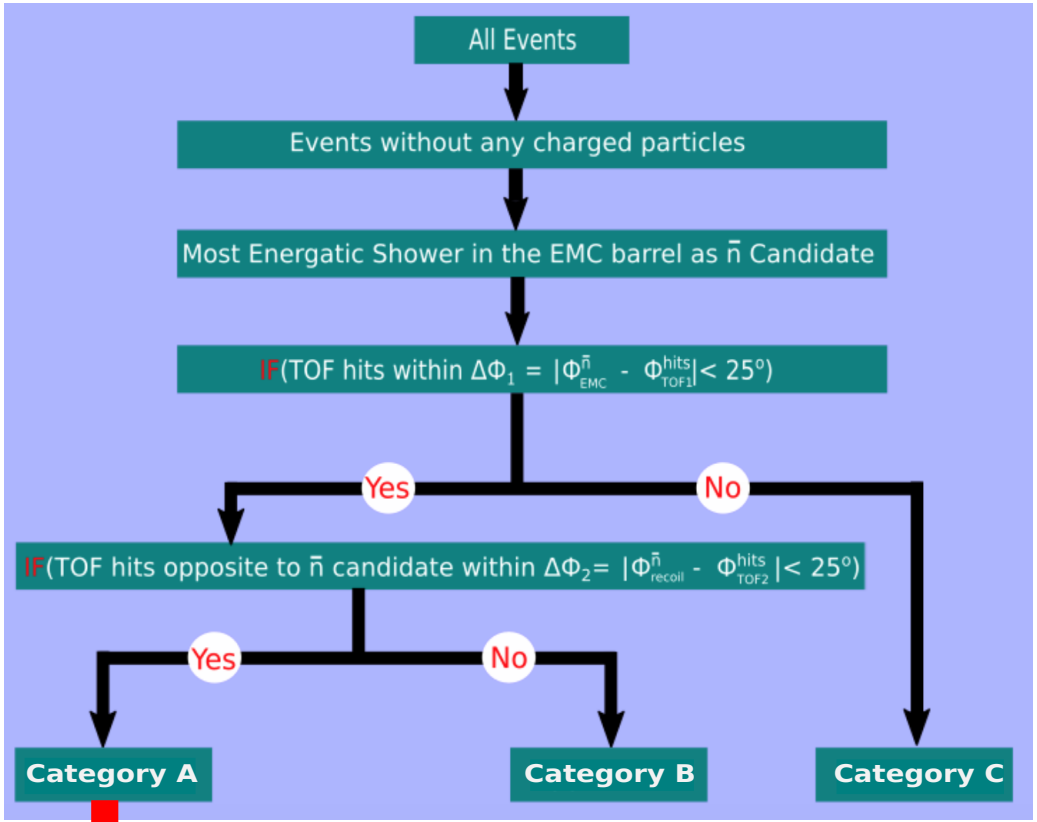

Selection	Value	Expression
$N_{charged}$	0	number of charged tracks without constraint on the vertex
$E_{\bar{n}}$	[0.5, 2.0] GeV	energy deposition of antineutron candidate (EMC1)
N^{50}_{HIT}	[30, 140]	number of hits in 50^o cone around antineutron
$\cos\theta$	[-0.7, 0.7]	cosine of polar angle of antineutron
$\Delta\phi_{(TOF1,EMC1)}$	[$-3\phi_c$, $3\phi_c$] rad.	azimuthal constraints on antineutron
$\theta_{(TOF1,EMC1)}$	[-0.5, 0.5] rad.	crossing angle between EMC1 and TOF1 for antineutron
$\Delta\phi_{(TOF2,EMC1)}$	[$-6\phi_c$, $6\phi_c$] rad.	azimuthal constraints on neutron
ΔT_n	[-4, 4] ns	the measured time difference from the expected for neutron
E_n	(, 0.7) [0.06, 0.7] GeV	energy deposition in EMC2 of neutron
$\theta_{TOF2',EMC1}$	3.0 [2.98] rad.	crossing angle between TOF2' of neutron and EMC1 of antineutron
ΔT	[-4.0, 4.0] ns	time difference between TOF2' of neutron and TOF1 of antineutron
$\theta_{EMC2,EMC1}$	[3.0,] rad.	crossing angle between EMC2 of neutron and EMC1 of antineutron

Category A

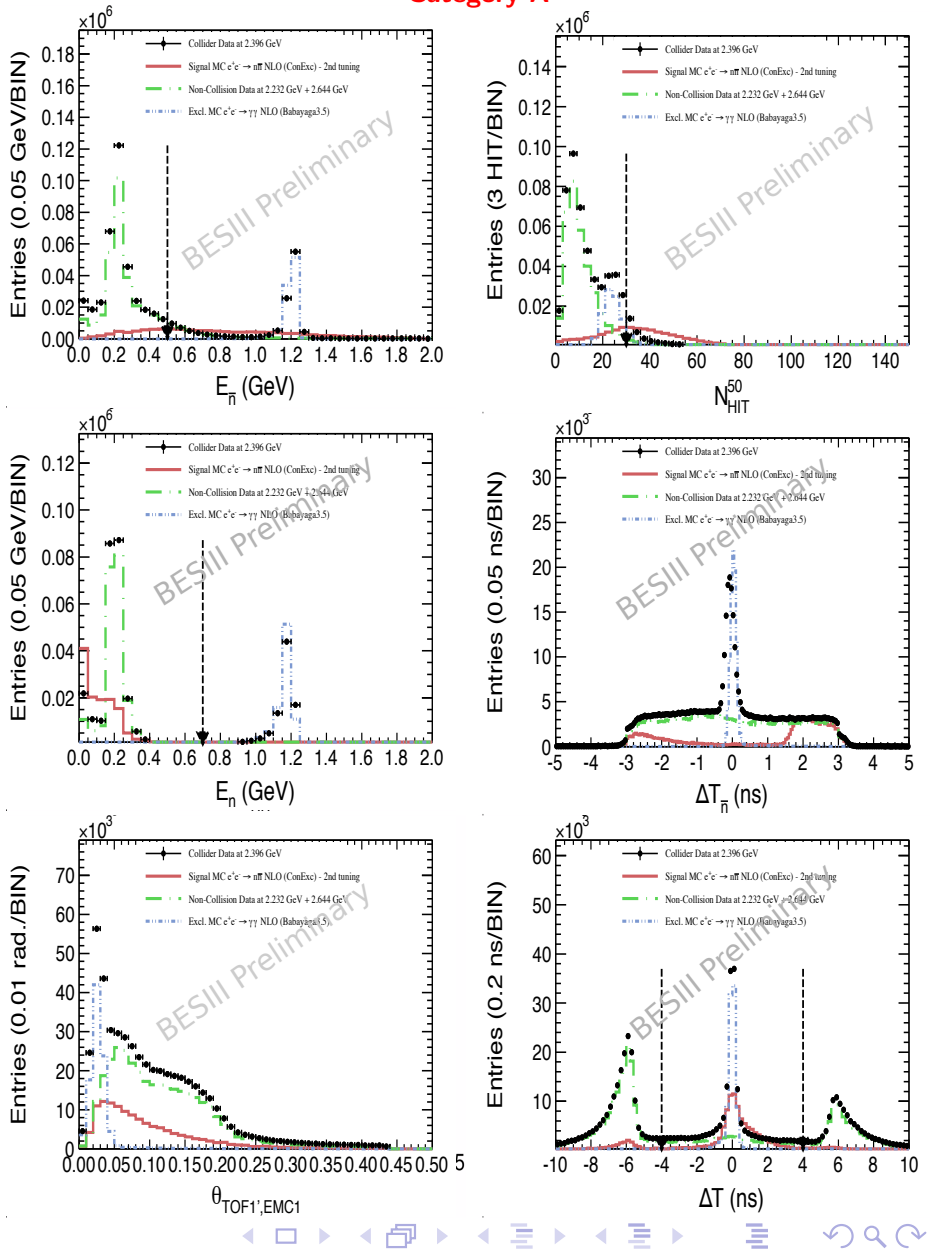

Analysis Strategy

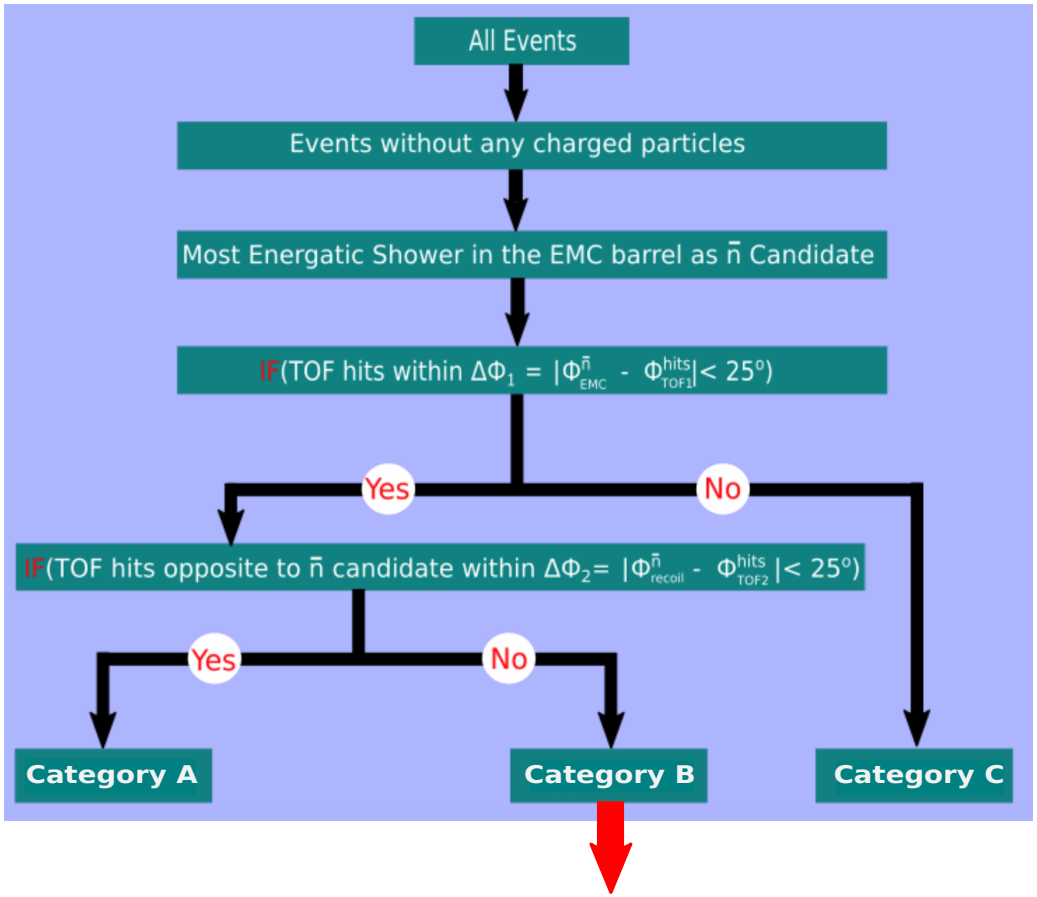

Selection	Value	Expression
$N_{charged}$	0	number of charged tracks without constraint on the vertex
$E_{\bar{n}}$	[0.5, 2.0] GeV	energy deposition of antineutron candidate (EMC1)
$\cos\theta$	[-0.7, 0.7]	cosine of polar angle of antineutron
$\Delta\phi_{(TOF1,EMC1)}$	[-3ϕ_c, 3ϕ_c] rad.	azimuthal constraints on antineutron
$\theta_{(TOF1,EMC1)}$	[-0.5, 0.5] rad.	crossing angle between EMC1 and TOF1 for antineutron
$\lvert\Delta T_\gamma\rvert$	> 0.5 ns	the measured time difference in hypothesis of photon
BDT	> 0.1	the BDT discriminator with seven $\bar{n}$ related variables
E_n	[0.04/0.06, 0.6] GeV	energy deposition of neutron candidate ($\sqrt{s} \leq$ / $>$ 2.3094 GeV
ll_{muc}	< 6	last layer with hits in the MUC
$\sphericalangle^n_{\bar{n}}$	$> 150^\circ$	opening angle between the n and n̄ candidate in the calorimeter

Category B

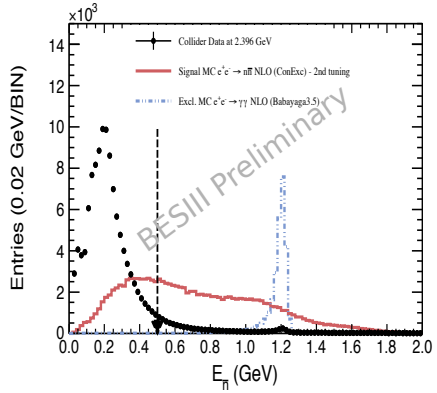

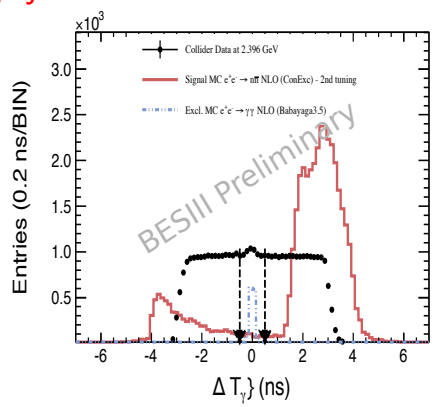

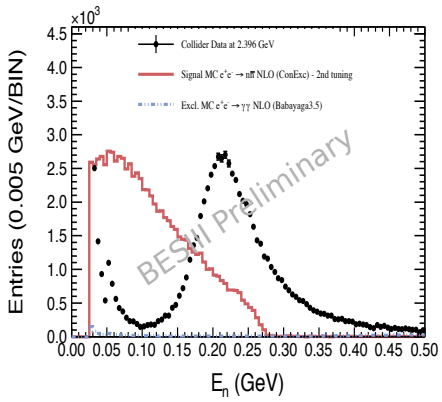

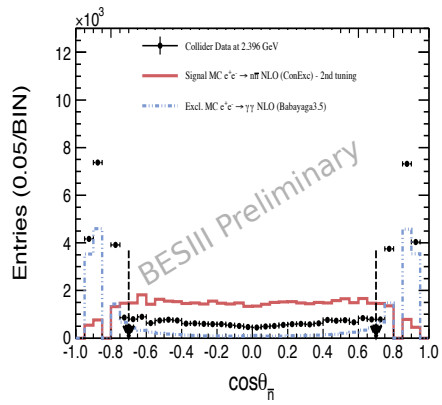

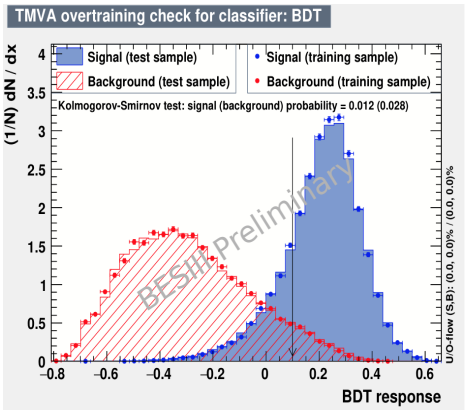

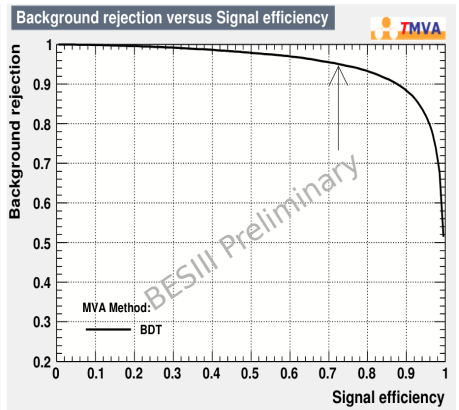

Analysis Strategy

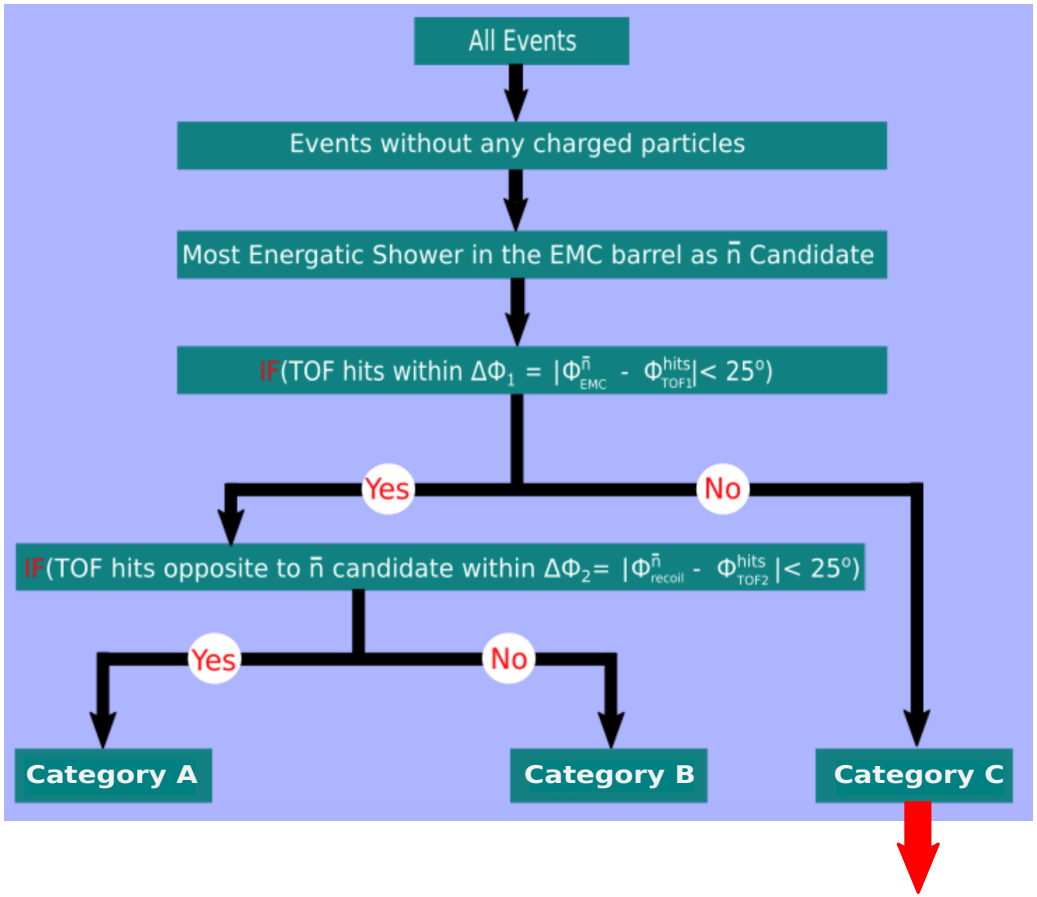

Selection	Value	Expression
$N_{charged}$	== 0	number of charged tracks without constrain on the vertex
$E_{\bar{n}}$	[0.5, 2.0] GeV	energy deposition of antineutron candidate in the calorimeter
2 $moment_{\bar{n}}$	>20 cm^2	second moment of antineutron candidate, 2 $moment_{\bar{n}} = \sum_i E_i r_i^2 / E_i$
N^{50}_{HIT}	[35, 100]	number of hits in 50^o cone around the n̄ candidate
E_n	[0.04/0.06, 0.6] GeV	energy deposition of neutron candidate ($\sqrt{s} \leq$ / > 2.3094 GeV
E_{extra}	<0.15 GeV	$E_{extra} = E_{total} - E^{50^o cone}_{\bar{n}} - E^{20^o cone}_{n}$
ll_{muc}	< 6	last layer with hits in the MUC
$\sphericalangle^{n}_{\bar{n}}$	> 150^o	opening angle between the n and n̄ candidate in the calorimeter

Category C

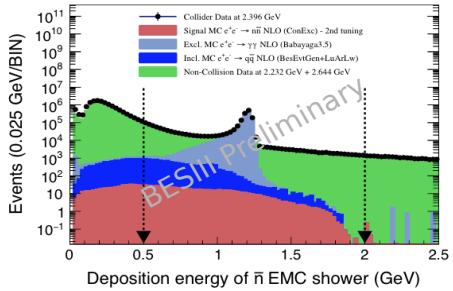

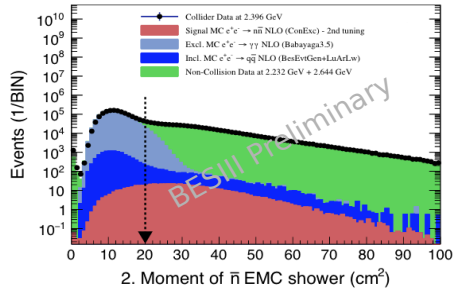

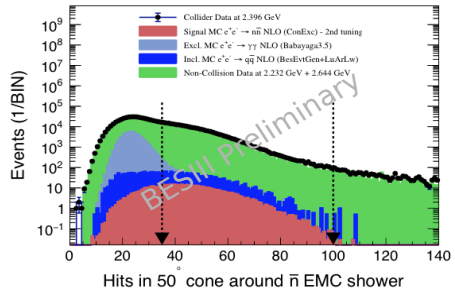

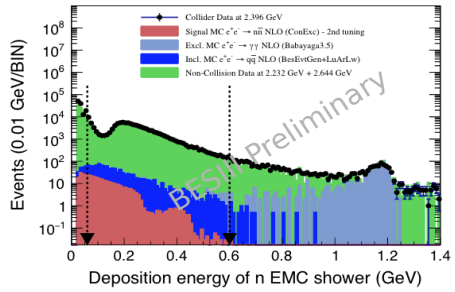

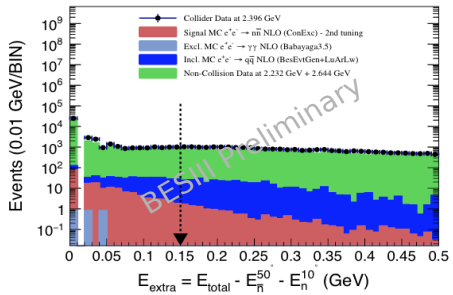

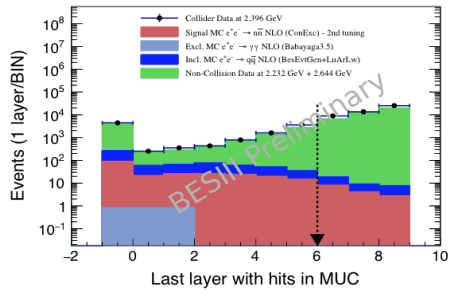

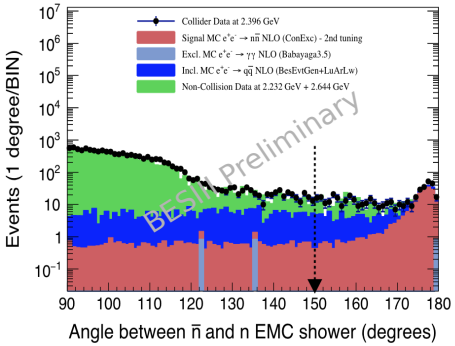

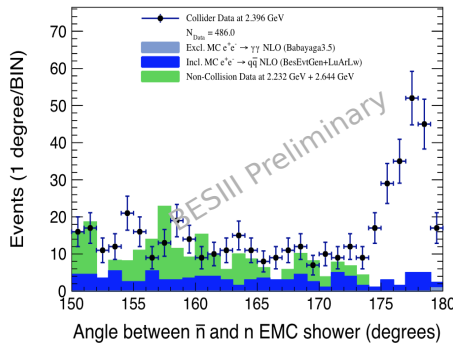

Extraction of Signal Yield

- **The signal yields in the 3 categories are extracted by the fit where the variables used for the fit:**

Category A: $(EMC+TOF)_{\bar{n}}+(TOF)_n$

Category B: $(EMC+TOF)_{\bar{n}}+(EMC)_n$

Category C: $(EMC)_{\bar{n}}+(EMC)_n$

$$\Delta T_n \equiv T_{TOF2} - T_0^n - T_n$$

$$T_n = \frac{L}{\beta C}, \beta = \frac{\sqrt{E_{cm}^2 - m^2}}{E_{cm}}$$

$$\theta_{n,\bar{n}} \equiv \arccos\left(\frac{V_{EMC1} \cdot V_{EMC2}}{|V_{EMC1}||V_{EMC2}|}\right)$$

Category A

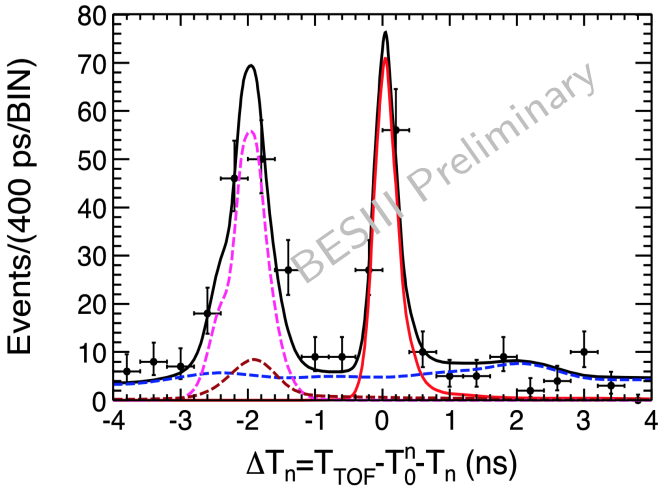

- Signal PDF: MC shape.
- Background PDF: data.

Category B

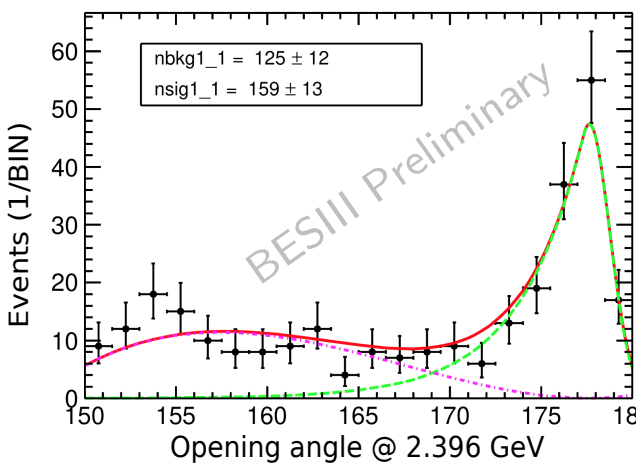

- Signal PDF: Crystal-ball function.
- Background PDF: three-order polynomial function.

Category C

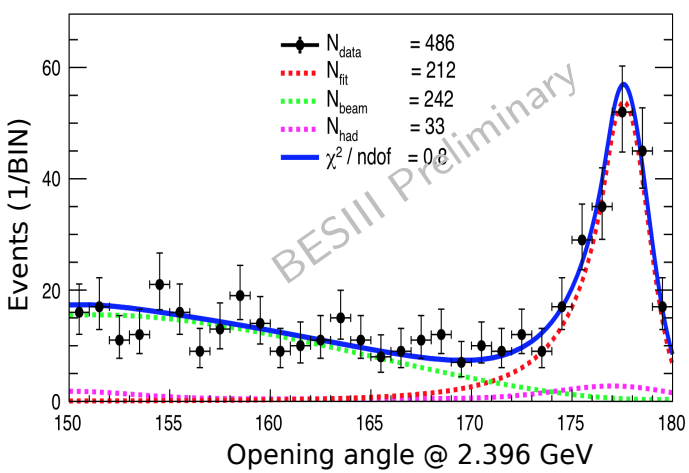

- Signal PDF: Crystal-ball function.
- Background PDF: Chebychev polynomial function of third order.

Born Cross Section and Effective Form Factors

- Experimentally, the Born cross section of the $e^+e^- \to n\bar{n}$ process is determined via:

$$\sigma_{Born} = \frac{N_{data}}{\epsilon_{n\bar{n}}^{MC} \times \mathcal{C}_{dm} \times \mathcal{C}_{trg} \times (1+\delta) \times \mathcal{L}_{Int}}$$

N_{data}: Number of selected $n\bar{n}$ data events, $\mathcal{C}_{dm}$: data/MC efficiency correction, $\mathcal{C}_{trg}$: trigger efficiency correction.

$1+\delta$: Radiative correction and vacuum polarisation $(1+\delta)$, $\epsilon_{n\bar{n}}^{MC}$: MC Efficiency, $\mathcal{L}_{Int}$: Luminosity

- Theoretically, the Born cross section of the $e^+e^- \to n\bar{n}$ is expressed in this form:

$$\sigma_{Born} = \frac{4\pi\alpha^2\beta}{3q^2}[|G_M|^2 + \frac{2m_n^2}{q^2}|G_E|^2]$$

- The effective form factor is defined as a linear compination of G_E and G_M FFs which is proportional to the square root of the nucleon pair production cross section:

$$|G_{eff}| = (\frac{3q^2}{4\pi\alpha^2\beta(1+\frac{2m_n^2}{q^2})})^{\frac{1}{2}}\sqrt{\sigma_{Born}}$$

Theoretically, $|G_{eff}|^2 = [|G_M|^2 + (\frac{2m_n^2}{q^2})|G_E|^2]/[1+\frac{2m_n^2}{q^2}]$

Results of Born Cross Section and Effective Form Factor

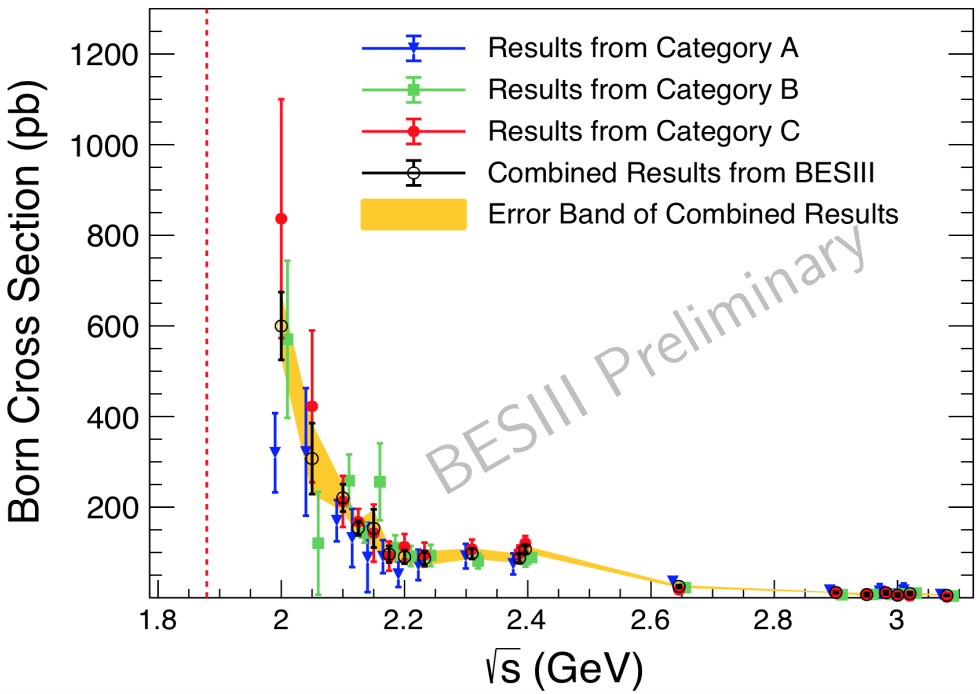

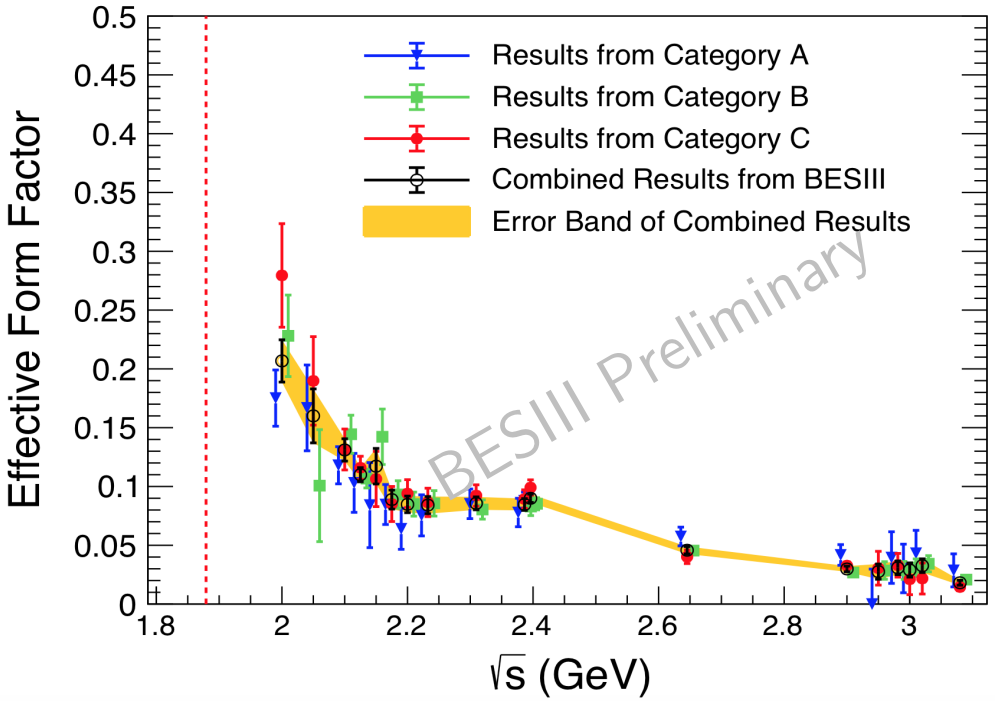

Results of the $e^+e^- \to n\bar{n}$ Born Cross Section:

- **The results from the three categories are in agreement within the error bars**.
- The combined cross sections are determined via:

$$\sigma_{BORN} = w_A\sigma_A + w_B\sigma_B + w_C\sigma_C, \quad \Delta\sigma_{BORN} = \left(\frac{1}{\sum_i (1/\Delta\sigma_i^2)}\right)^{\frac{1}{2}}, \quad w_i = \frac{1/\Delta\sigma_i^2}{\sum_i (1/\Delta\sigma_i^2)}, \quad i = A, B, C.$$

σ_i and $\Delta\sigma_i$ are the cross sections and their error bars, respectively.

Angular Analysis for the Extraction of R_{em} and $|G_M|$ FFs

- The R_{em} and $|G_M|$ form factors can be extracted by fitting the efficiency corrected angular distribution:

$$\frac{d\sigma^{Born}_{n\bar{n}}}{dcos\theta_{\bar{n}}} = \frac{d\mathcal{N}/dcos\theta_{\bar{n}}}{\epsilon^{MC}_{n\bar{n}} \times \mathcal{C}_{dm} \times \mathcal{C}_{trg} \times (1+\delta) \times \mathcal{L}_{Int}} = A \times |G_M|^2 \left[(1+cos^2\theta_{\bar{n}}) + R^2_{em}\frac{4M_n^2}{s}(1-cos^2\theta_{\bar{n}})\right]$$

  - $R^2_{em} = |G_E/G_M|$ is the form factor ratio, $A = \frac{2\pi\alpha^2\beta}{4s}$ is the normalisation factor.

- Integration over bin width of the fit function is performed due to the large bin width:

$$\left(\frac{d\sigma^{Born}_{n\bar{n}}}{dcos\theta_{\bar{n}}}\right)_i = \sum_{bin=1}^{bin=n} \int_{bin} A_i \times |G_M|^2 \left[(1+cos^2\theta_{\bar{n}}) + R^2_{em}\frac{4M_n^2}{s}(1-cos^2\theta_{\bar{n}})\right]$$

  - i stands for the three categories, i.e A, B and C.

- **The neutron form factors are extracted by performing a simultaneous fit to the angular distributions from the three categories where the R_{em} is shared.**

Estimation of Systematic Uncertainties

- **All expected sources of systematic uncertainties have been studied:**

Cross Section and EFF:
- Luminosity
- All individual selection criteria
- Fit for signal yield extraction (fit range, signal and background model)
- Trigger efficiency
- Radiative corrections
- Iterative MC tuning

Form Factor Ratio
- Differential selection
- Differential signal yield extraction (range, signal and background model)
- Bin width
- Angular fit range

Magnetic Form Factor
- Differential selection
- Differential signal yield extraction (range, signal and background model)
- Luminosity
- Trigger efficiency
- Radiative corrections
- Iterative MC tuning

- **The results for the cross section, the form factor ratio and the magnetic form factor are dominated by the statistical uncertainties.**

BESIII Experiment

Beijing Electron Positron Collider II and BESIII Detector

Beijing Electron Positron Collider

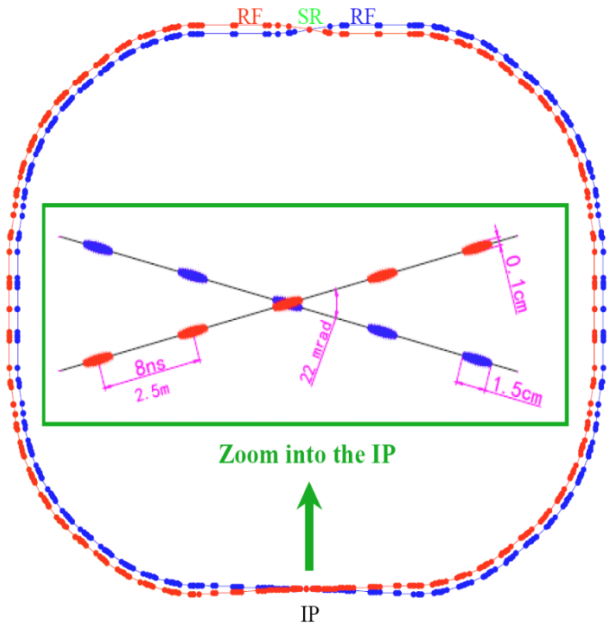

- Symmetric e^+e^- collider
- Beam energy: 1.0 - 2.3 GeV
- Optimum energy: 1.89 GeV
- Design luminosity: 10^{33} cm^{-2} s^{-1}
- Crossing angle: 22 mrad

BESIII detector

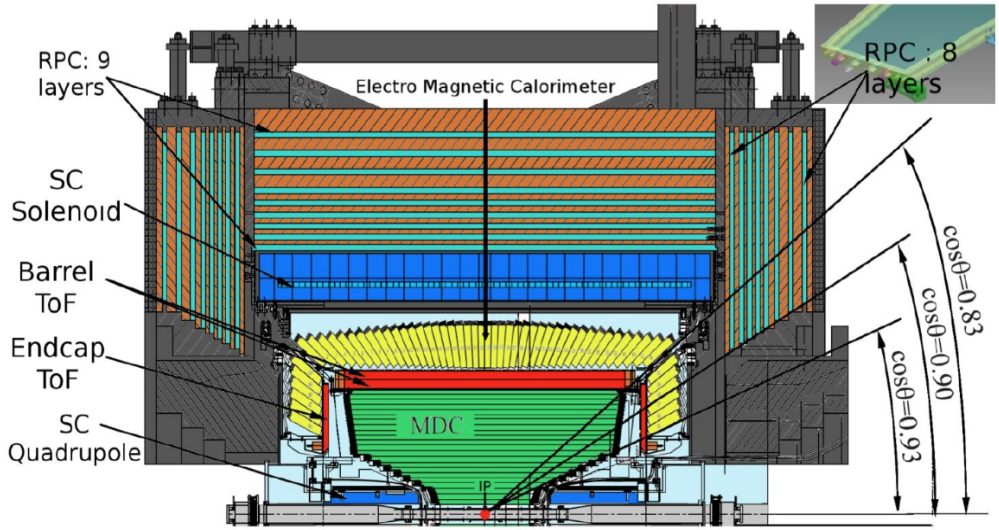

Electromagnetic Calorimeter
$\sigma_E/\sqrt{E}(\%)$=2.5% (1 GeV),
(CsI) $\sigma_{z,\phi}$(cm)=0.5-0.7 cm/$\sqrt{E}$

Muon Counter
σ_{xy}<2 cm

Time Of Flight
σ_T(barrel)=90 ps
σ_T(endcap)=110 ps

Main Drift Chamber
σ_{xy}=130 mm, dE/dx~6%
σ_p/p = 0.5% at 1 GeV

BESIII Data Sets and Physics Program

- World largest data samples for J/ψ, ψ' and ψ''

- Charm physics
- Charmonium spectroscopy
- Light hadrons
- New physics research
- Form factors measurements
- ....

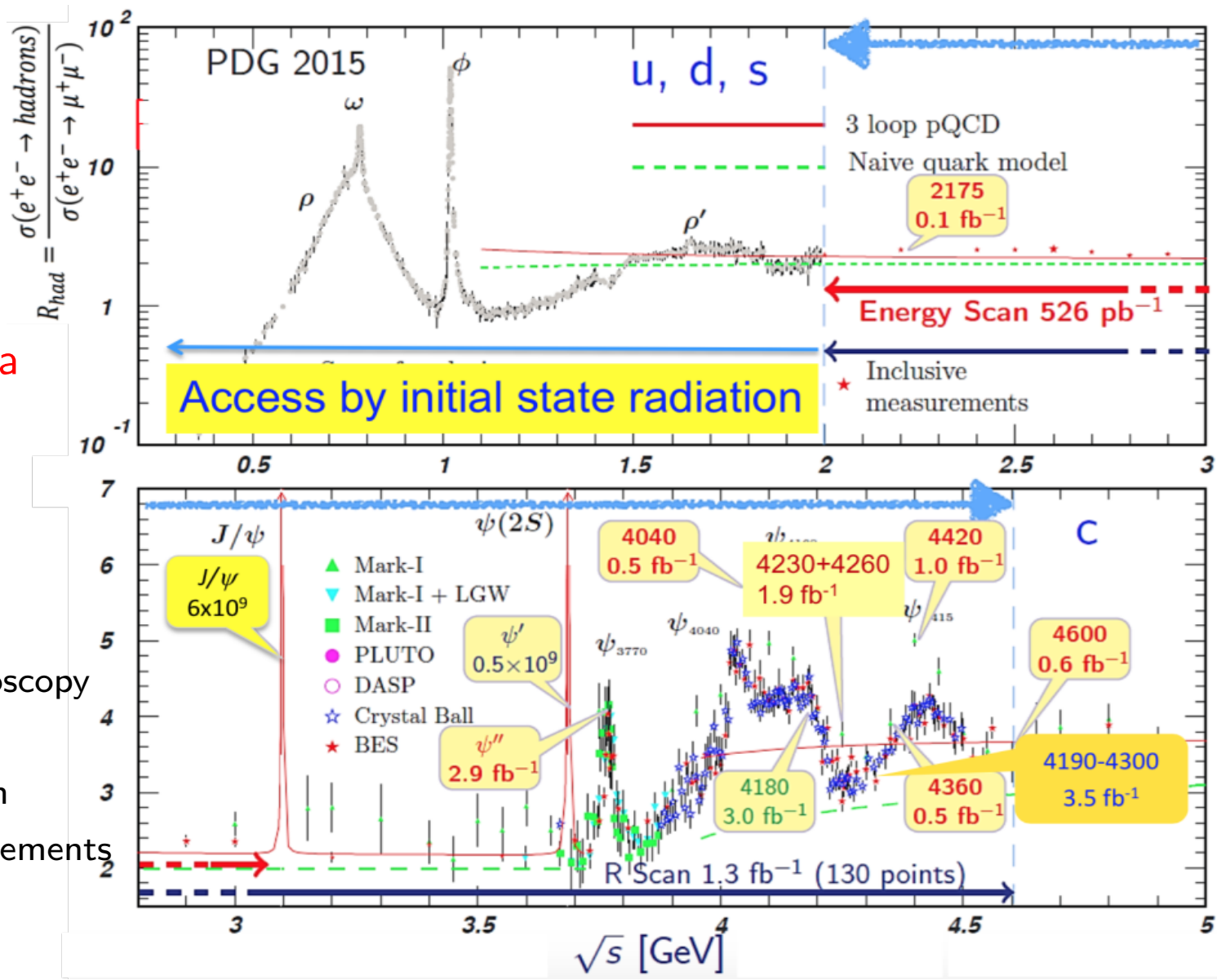

Proton results

Structure in the Effective Form Factor of the Proton

- Oscillation in the effective form factor is observed by BaBar and then confirmed by BESIII.

PRL114,232301- PRC93,035201

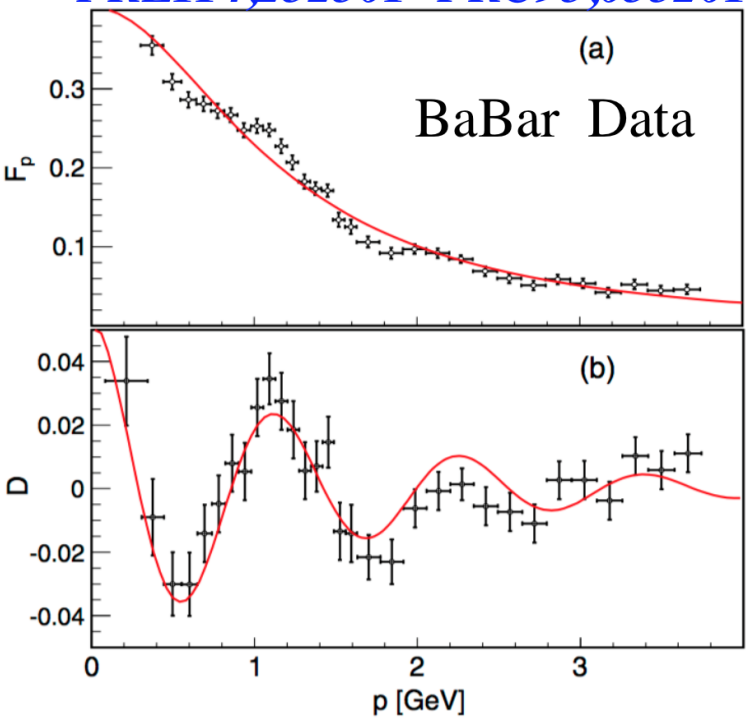

$$F_{\mathrm{osc}}(p) \equiv A\exp(-Bp)\cos(Cp+D)$$

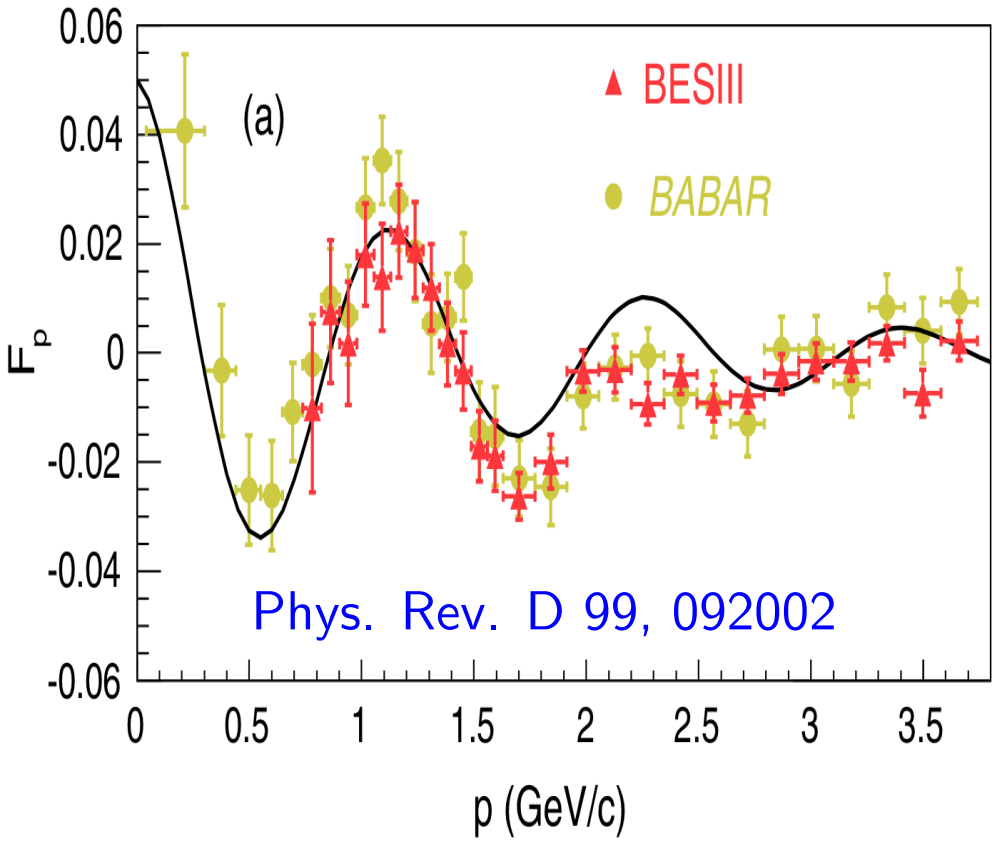

- A physical explanation could be due to a possible interference effect involving rescattering processes at moderate kinetic energies of the outgoing hadrons (when the center-of-mass of the produced hadrons are separated by 1 fm)

p is the three momentum of the proton in the frame of antiproton.

Measurements of Proton Form Factors at BESIII

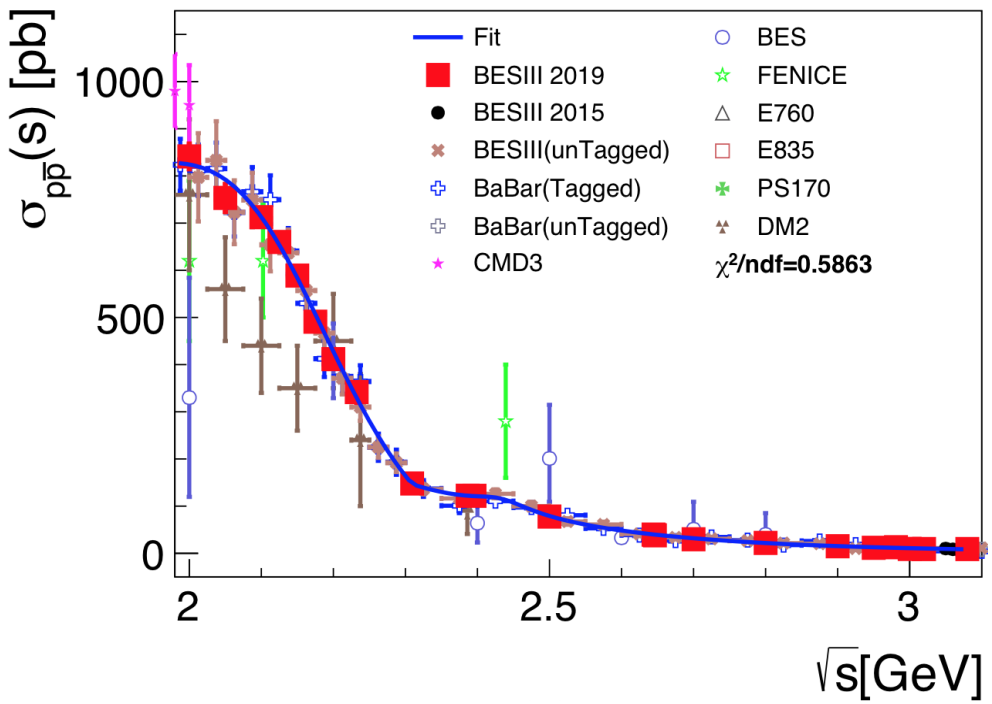

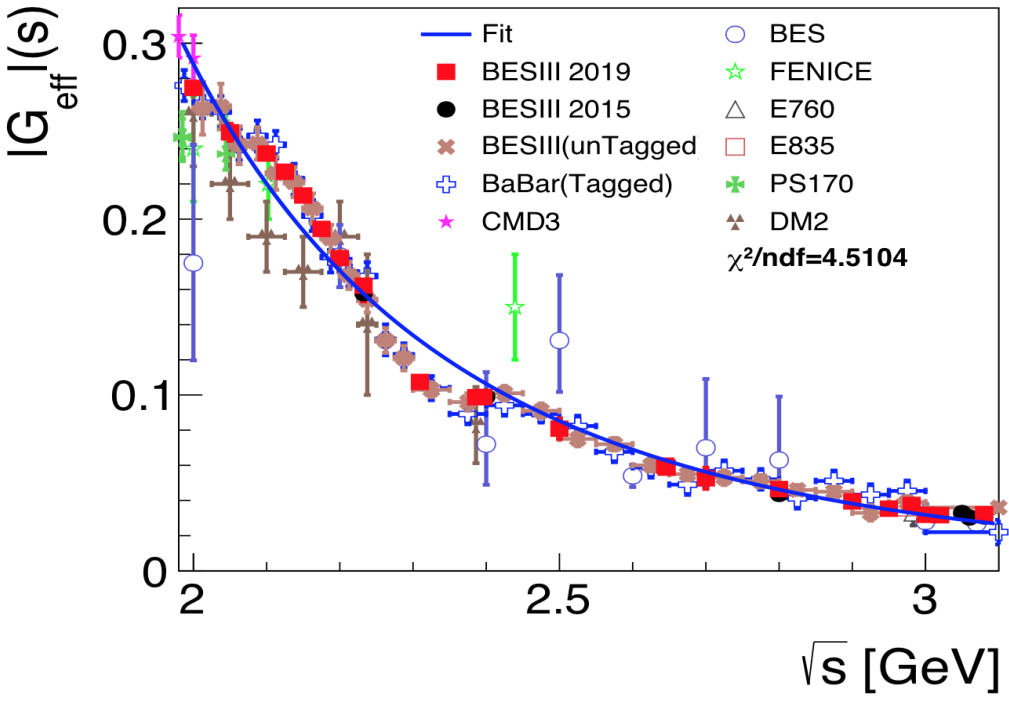

BESIII results for the $e^+e^- \to p\bar{p}$ cross section and effective form factors

- Direct scan method:
  - 2012 data, 156.7 pb^{-1}, 12 c.m energies, Phys. Rev. D 91, 112004 (2015)
  - 2015 data, 668.5 pb^{-1}, 22 c.m energies, arXiv:1905.09001 $\Longrightarrow$ most precise results.
- Initial state radiation method:
  - Untagged analysis: data at [3.773 - 4.60 GeV], 7.4 pb^{-1}, Phys. Rev. D 99, 092002;
  - Tagged analysis: data at [3.773 - 4.60 GeV], 7.4 pb^{-1}, under review ;